Deep residual networks for wireless transmitter localization using sparse boundary measurements

by

Arash AHMADI

MANUSCRIPT-BASED THESIS PRESENTED TO ÉCOLE DE TECHNOLOGIE SUPÉRIEURE
IN PARTIAL FULFILLMENT OF A MASTER'S DEGREE
WITH THESIS IN ELECTRICAL ENGINEERING
M.A.Sc.

MONTREAL, DECEMBER 5, 2025

ÉCOLE DE TECHNOLOGIE SUPÉRIEURE
UNIVERSITÉ DU QUÉBEC

BOARD OF EXAMINERS

THIS THESIS HAS BEEN EVALUATED

BY THE FOLLOWING BOARD OF EXAMINERS

Professor Richard Al Hadi, Thesis supervisor
Department of Electrical Engineering, École de technologie supérieure

Professor Camille Coti, Chair, Board of Examiners
Department of Software Engineering and IT, École de technologie supérieure

Professor Kim Khoa Nguyen, Member of the Jury
Department of Electrical Engineering, École de technologie supérieure

THIS THESIS WAS PRESENTED AND DEFENDED

IN THE PRESENCE OF A BOARD OF EXAMINERS AND THE PUBLIC

ON NOVEMBER 5, 2025

AT ÉCOLE DE TECHNOLOGIE SUPÉRIEURE

ACKNOWLEDGEMENTS

I sincerely express my deepest gratitude to my supervisor, Professor Richard Al Hadi, for his unwavering guidance, continuous support, and invaluable encouragement throughout this research. His expertise and dedication have been instrumental in shaping the direction and outcome of this work.

I would also like to extend my heartfelt gratitude to my family, including my mother, father, brother, and sister-in-law, for their wholehearted support, patience, and encouragement during this journey. Their belief in me, combined with their constant motivation, has been a source of strength and perseverance, making this achievement possible.

Lastly, I would like to acknowledge the contribution of the late Professor Charles Despins for the project initiation.

This research was enabled in part by support provided by Calcul Québec (calculquebec.ca) and the Digital Research Alliance of Canada (alliancecan.ca).

Réseaux résiduels profonds pour la localisation des émetteurs sans fil à l'aide de mesures de frontière éparses

Arash AHMADI

RÉSUMÉ

La localisation des émetteurs est un défi crucial en communication sans fil, influençant l'optimisation des réseaux, la sécurité et la gestion du spectre. Les techniques de localisation traditionnelles, telles que la triangulation et la méthode d'empreinte numérique du signal (fingerprinting), nécessitent une collecte de données intensive et des ressources computationnelles importantes, les rendant peu pratiques pour des déploiements à grande échelle. Cette thèse explore une méthode de localisation basée sur l'apprentissage profond, exploitant un réseau neuronal résiduel (ResNet) pour prédire la position d'un émetteur sans fil à partir de mesures de puissance du signal prises aux limites de la zone d'intérêt. Contrairement aux approches conventionnelles qui reposent sur une collecte complète des données sur toute la zone, la méthode proposée réduit considérablement la complexité des mesures tout en maintenant une précision élevée. Le modèle est entraîné sur un ensemble de cartes de propagation radio simulées à l'aide du modèle de chemin dominant (Dominant Path Model - DPM) et évalué sur des scénarios de mesures synthétiques et réels. Les résultats expérimentaux montrent une erreur moyenne de localisation de 7,23 mètres avec un écart type de 3,32 mètres, ce qui le rend compétitif par rapport aux techniques de localisation par apprentissage profond les plus avancées. De plus, une métrique de confiance est introduite pour évaluer la fiabilité des prédictions dans des conditions sans ligne de vue. Ces résultats soulignent le potentiel de l'apprentissage profond résiduel pour une localisation des émetteurs rentable dans des environnements complexes avec un accès limité aux mesures. Cette recherche contribue au développement de solutions efficaces basées sur l'apprentissage automatique pour l'analyse des signaux sans fil, ouvrant la voie à une meilleure gestion des réseaux et des stratégies d'atténuation des interférences.

Mots-clés: fréquence radio, carte de propagation, apprentissage profond, réseaux résiduels, réseaux de neurones convolutionnels, localisation du signal

Deep residual networks for wireless transmitter localization using sparse boundary measurements

Arash AHMADI

ABSTRACT

Transmitter localization is a critical challenge in wireless communication, impacting network optimization, security, and spectrum management. Traditional localization techniques, such as triangulation and fingerprinting, require extensive data collection and computational resources, making them impractical for large-scale deployments. This thesis explores a deep learning-based localization method that leverages a Residual Neural Network (ResNet) to predict the position of a wireless transmitter using sparse boundary signal strength measurements. Unlike conventional methods that rely on full-area data collection, the proposed approach significantly reduces measurement complexity while maintaining high localization accuracy. The model is trained on a dataset of simulated radio propagation maps generated using the Dominant Path Model (DPM) and evaluated on both synthetic and real-world measurement scenarios. Experimental results demonstrate an average localization error of 7.23 meters, with a standard deviation of 3.32 meters, making it competitive with state-of-the-art deep learning localization techniques. Additionally, a confidence metric is introduced to assess prediction reliability in non-line-of-sight conditions. The findings highlight the potential of deep residual learning for cost-effective transmitter localization in complex environments with limited access. This research contributes to the development of deep learning solutions for wireless signal analysis, paving the way for enhanced network management and interference mitigation strategies.

Keywords: radio frequency, propagation map, deep learning, residual networks, convolutional neural networks, signal localization

TABLE OF CONTENTS

Page

INTRODUCTION 1

CHAPTER 1 LITERATURE REVIEW 7
1.1 Localization Methods 7
1.1.1 Fingerprinting 7
1.1.2 Triangulation 9
1.2 Deep Learning in Localization 10
1.2.1 CNN-Based Models 10
1.2.2 Reinforcement Learning-Based Approaches 11
1.2.3 ResNet for Localization 12
1.3 Research Gap 13

CHAPTER 2 A RESIDUAL NEURAL NETWORK APPROACH TO TRANSMITTER LOCALIZATION 15
2.1 Introduction 16
2.2 Methodology 18
2.2.1 Description of ResNet and its benefits 20
2.2.2 RadioMapSeer Dataset 22
2.3 Model Training 24
2.3.1 Training Procedure 24
2.3.2 Performance on Test Data 25
2.3.3 Remedy for outliers scenarios 28
2.4 Measurements 33
2.4.1 Setup for Measurements 33
2.4.2 Data Collection Process 34
2.4.3 Results 34
2.5 Discussion 35
2.5.1 Comparison with State-of-the-Art 35
2.5.2 Ablation and Generalization Study 38
2.5.2.1 Unknown Tx Power 39
2.5.2.2 Sparser Measurements 39
2.5.2.3 Dataset Augmentation 40
2.5.2.4 Measurements from Two Borders 41
2.5.2.5 Separate Layouts in Training and Test 41
2.5.3 Practical Considerations and Limitations 42
2.6 Conclusion 42

CONCLUSION AND RECOMMENDATIONS 45

ANNEX A WIRELESS NETWORK DEPLOYMENT SURVEY 49

ANNEX B UNET-BASED DEEP LEARNING PATHLOSS ESTIMATOR WITH BOUNDARY CONDITION INPUT 59

LIST OF REFERENCES 71

LIST OF TABLES

Page

Table 2.1 Comparison of TxLocNet performance with different deep learning architectures 26

Table 2.2 Localization performance of TxLocNet across different confidence-index thresholds 30

Table 2.3 TxLocNet accuracy using measurements at various locations 35

Table 2.4 Comparison with state-of-the-art 36

Table 2.5 Effect of interpolation on TxLocNet performance 40

LIST OF FIGURES

Page

Figure 0.1 Number of papers listed in Scopus that include "signal localization" in their titles 1

Figure 1.1 Fingerprinting-based localization process 7

Figure 1.2 Localization of a rogue access point using triangulation 9

Figure 1.3 Structure of a conventional CNN 11

Figure 1.4 A localization method based on reinforcement learning 12

Figure 1.5 Building block of a ResNet 13

Figure 2.1 Task overview: the transmitter is located inside the area of interest, while signal strength measurements are collected along the accessible border, following a straight path 19

Figure 2.2 TxLocNet overview: border measurements as input vector, ResNet-based inference model, predicted transmitter location coordinates as output 21

Figure 2.3 Dataset: Path loss maps from RadioMapSeer; boundary vectors from path loss maps (input for TxLocNet), corresponding Tx locations (target for TxLocNet) 24

Figure 2.4 The percentage histogram of TxLocNet localization error on test dataset of 8,412 images 27

Figure 2.5 Scenarios where TxLocNet predicts the Tx location with high errors 28

Figure 2.6 Scatter plot of TxLocNet error on the test data along x- and y-axis. The color gradient showcase the amount of confidence index 30

Figure 2.7 Top: path loss map of a scenario where the signal from the transmitter is obstructed by obstacles; bottom: TxLocNet error and confidence index vs measurement path position 32

Figure 2.8 Aerial views of the measurement locations 33

Figure 2.9 Euclidean Error vs. Assumed Tx power 39

LIST OF ABBREVIATIONS

ETS	École de Technologie Supérieure
6G	Sixth Generation Wireless Networks
IoT	Internet of Things
D2D	Device-to-Device
ResNet	Residual Neural Network
NLoS	Non-Line-of-Sight
CNN	Convolutional Neural Network
RSS	Received Signal Strength
SDR	Software-Defined Radio
AoA	Angle of Arrival
ToA	Time of Arrival
RL	Reinforcement Learning
3D	Three-Dimensional
IEEE	Institute of Electrical and Electronics Engineers
RSSI	Received Signal Strength Indicator
ML	Machine Learning
LoS	Line-of-Sight
FSPL	Free Space Path Loss
MSE	Mean Squared Error

DPM	Dominant Propagation Model
GS	Gray-Scale
EARFCN	E-UTRA Absolute Radio Frequency Channel Number
E-UTRA	Evolved UMTS Terrestrial Radio Access]
UMTS	Universal Mobile Telecommunications System
RSRP	Reference Signal Received Power
LTE	Long-Term Evolution
WSN	Wireless Sensor Network
SotA	State-of-the-Art
OOD	Out-of-Distribution
USRP	Universal Software Radio Peripheral
AI	Artificial Intelligence
RF	Radio Frequency
5G	Fifth Generation Wireless Networks
Wi-Fi	Wireless Fidelity
AP	Access Point
BIM	Building Information Modeling
BPSK	Binary Phase Shift Keying
CW	Continuous Wave
EM	Electromagnetic

ETS	École de Technologie Supérieure
LNA	Low Noise Amplifier
MEP	Mechanical, Electrical, and Plumbing
PDP	Power Delay Profile
VNA	Vector Network Analyzer
Tx	Transmitter
Rx	Receiver

LIST OF SYMBOLS AND UNITS OF MEASUREMENTS

m	meters
km	kilometers
m^2	square meters
km^2	square kilometers
Hz	hertz
kHz	kilohertz
MHz	megahertz
GHz	gigahertz
dB	decibels
dBm	decibel-milliwatts
px	pixels
ns	nanoseconds
mA	milliamperes
V	volts

INTRODUCTION

The rapid growth of wireless communication systems has made the accurate localization of transmitters a critical component for efficient network management and robust system performance. Signal source localization has been a hot topic in research circles, particularly since the 1990s, driven by advancements in wireless communication and positioning technologies. As Figure 0.1 illustrates, the growth in this area has been sustained at a high level since the 2010s, highlighting the field's continued relevance in modern telecommunications and emerging technologies.

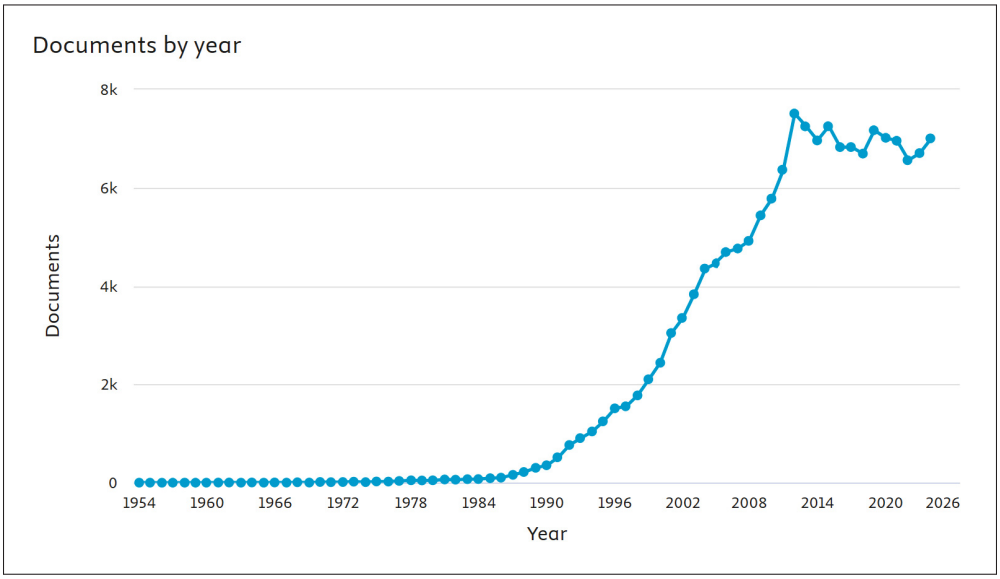

Figure 0.1 Number of papers listed in Scopus that include "signal localization" in their titles

Applications such as network optimization, interference mitigation, and public safety heavily depend on precise localization techniques. However, traditional methods like fingerprinting and triangulation face challenges in terms of feasibility, computational complexity, and adaptability to environments with limited access.

Context

Wireless localization has long been a foundational pillar for telecommunications and network engineering, enabling functions as diverse as emergency response (Lee, Kang, Jeong & Seo (2022)), rogue transmitter detection (Jagannath & Jagannath (2020)), and smart city infrastructure planning (Kuruvatti *et al.* (2022)). As global connectivity scales upward with the advent of 6G, IoT, and intelligent transportation systems, the need for robust, scalable localization techniques is becoming increasingly urgent. Current localization methods, though effective, face a multitude of challenges:

- **Fingerprinting** involves mapping the signal strength at numerous grid points within an area (Bahl & Padmanabhan (2000)). This approach demands extensive data collection, which becomes infeasible in large-scale or frequently changing environments. Moreover, fingerprinting lacks generalizability when the physical characteristics of an environment are altered.
- **Triangulation** relies on calculating the angles and distances between a transmitter and multiple receivers (Osa, Matamales, Monserrat & López (2013)). While simple in theory, its performance degrades in environments characterized by significant signal reflection, refraction, and obstruction, such as dense urban areas or settings with complex layouts.
- **Machine learning-based localization** techniques have also been employed for signal localization (Nurminen, Dashti & Piché (2017)); however, they typically require measurement data from multiple locations throughout the map to achieve reliable generalization. Their accuracy declines when limited to sparse data gathered along a single trajectory, as they struggle to account for spatial variations across the entire environment. This strong reliance on extensive data collection reduces their practicality, especially in large or restricted-access areas where obtaining comprehensive measurements is challenging.

In preparation for the development of a signal localization framework, an initial study (see Annex A) was conducted to assess the reliability of radio wave propagation modeling tools. This work, presented as a conference paper titled "Wireless Network Deployment Survey", focused on validating electromagnetic (EM) simulation results against real-world measurements. To enhance the accuracy of generated radiomaps, this study utilized Building Information Modeling (BIM) within RF propagation simulation software and evaluated the reliability of these simulations by comparing them against real-world on-site measurements. Measurements conducted in an indoor environment demonstrated the feasibility of using BIM-enabled simulations to characterize wireless channel properties accurately.

Following the evaluation of simulation-based radio maps, a subsequent study (see Annex B) explored the possibility of extending propagation maps using deep learning techniques without requiring prior knowledge of the transmitter's location. This research, documented in a conference paper titled "UNet-Based Deep Learning Pathloss Estimator with Boundary Condition Input", introduced a UNet-based model that extends path loss radio maps using only border measurements. Unlike conventional approaches that rely on full knowledge of transmitter specifications and measurement points spread throughout the map, this framework demonstrated that meaningful spatial information could be inferred from limited inputs. The results confirmed that deep learning models could effectively capture the underlying propagation characteristics, supporting the feasibility of utilizing neural networks for localization with sparse data. These findings directly influenced the methodological choices for this thesis, particularly in leveraging deep residual networks (ResNets) for localization using minimal measurements along the border of an area of interest.

Aim of the Research

In response to the challenges of current localization methods, this thesis explores the application of deep learning to the problem of wireless transmitter localization. By leveraging only signal

strength measurements collected at the borders of an area of interest, the research aims to develop a novel localization framework that achieves comparable accuracy using low cost measurement equipment with limited measurements. Specifically, the objectives of this work are:

1. To demonstrate that meaningful spatial patterns can be extracted from sparse border measurements, circumventing the need for exhaustive signal mapping.
2. To establish the feasibility of utilizing Residual Neural Networks (ResNets) as an efficient and effective deep learning architecture for localization tasks.
3. To validate the model's applicability in real-world scenarios, including environments with significant multipath propagation and non-line-of-sight (NLoS) conditions.

Research Question

The research is driven by the following overarching question:

- Can border-only signal strength measurements, combined with deep learning, provide an accurate and efficient solution for wireless transmitter localization?

Methodology Overview

The methodology adopted in this research integrates theoretical, simulation-based, and experimental approaches to address the research question. The core aspects of the methodology include:

- **Data Generation:** This study utilizes a pre-existing dataset (Yapar, Levie, Kutyniok & Caire (2022)) of simulated radio maps generated using tools like WinProp, covering diverse urban environments. Each map includes path loss values and transmitter coordinates, with border measurements extracted as input features.
- **Model Architecture:** A ResNet-based model is designed and trained to map the border signal strength measurements to transmitter coordinates. ResNet's residual connections

facilitate the learning of complex spatial relationships in sparse datasets, improving both convergence and accuracy.

- **Experimental Validation:** The trained model is evaluated using simulated scenarios from Yapar *et al.* (2022) and real-world measurements collected in urban environments. These measurements include scenarios with significant environmental variability, such as obstructed paths and multipath effects.
- **Performance Metrics:** Model performance is assessed using metrics such as the mean and standard deviation of localization error, along with a confidence index that quantifies the model's certainty in its predictions based on the input data.

Thesis Structure

This thesis is organized as follows:

- **Chapter 1 - Literature Review:** A review of existing localization methods like fingerprinting and triangulation, along with deep learning approaches such as CNNs, reinforcement learning, and ResNets.
- **Chapter 2 - Main Article: A Residual Neural Network Approach to Transmitter Localization** A detailed presentation of the proposed methodology, experimental design, results, and analysis.

Finally, this manuscript concludes with a discussion of key findings, highlighting the effectiveness of the proposed ResNet-based localization approach. It explores practical applications, acknowledges limitations, and outlines future research directions, demonstrating the potential of deep learning for wireless transmitter localization.

Additionally, Annex A and Annex B are included to provide context and validation for the main research article presented in Chapter 2. Annex A, Wireless Network Deployment Survey, details an experimental study comparing electromagnetic simulations with real-world measurements.

This work establishes the reliability of the simulation tools and methodologies later used to generate the training datasets for the proposed ResNet-based localization framework. Annex B, UNet-Based Deep Learning Pathloss Estimator with Boundary Condition Input, presents a deep learning approach for extending propagation maps from sparse boundary measurements. The concepts, dataset processing methods, and insights from this study directly informed the architectural choices and measurement strategies adopted in the main article. Together, these annexes document the preliminary investigations that shaped the thesis methodology and validate the feasibility of the sparse-measurement approach central to the primary research study detailed in Chapter 2.

CHAPTER 1

LITERATURE REVIEW

1.1 Localization Methods

Localization of wireless transmitters is a fundamental challenge in wireless communication, with applications ranging from network planning to interference mitigation and spectrum monitoring. Several traditional approaches have been employed to estimate transmitter locations, including fingerprinting and triangulation. While these methods have seen extensive deployment, they present limitations in terms of scalability, accuracy, computational efficiency, and cost of required hardware.

1.1.1 Fingerprinting

Fingerprinting is a widely used approach that involves measuring and storing the received signal strength (RSS) or other signal characteristics at predefined locations within an environment. This database of measurements serves as a reference against which new observations can be compared to estimate a transmitter's location.

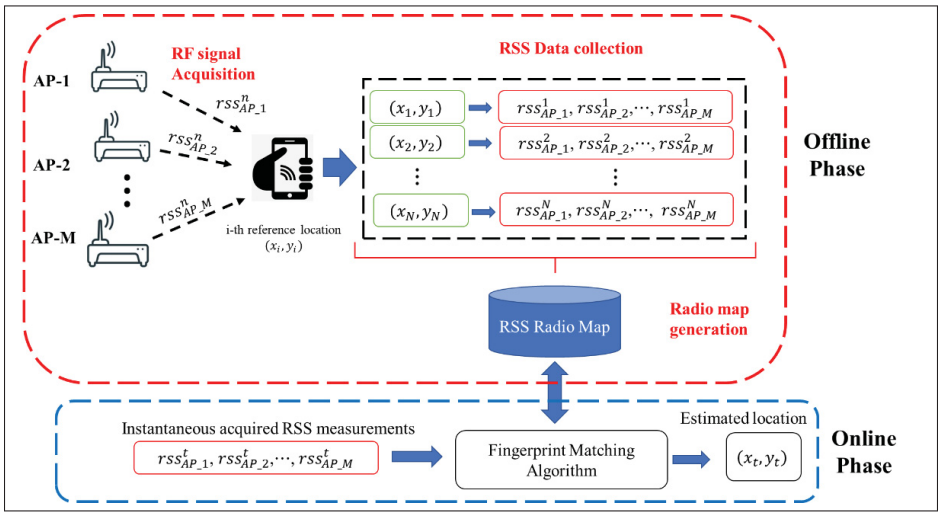

Figure 1.1 Fingerprinting-based localization process
Taken from Yaro *et al.* (2023)

The fingerprinting-based localization methods usually consists of two key stages: the offline phase and the online phase, as illustrated in Figure 1.1. During the offline phase, RF signals from wireless access points (APs) are captured using a smartphone at predefined reference points. The received signal strength (RSS) values for each detected RF signal are then measured and recorded. Finally, a radio map is generated, which serves as a database linking the RSS vectors to their corresponding coordinates.

Fingerprinting methods have demonstrated high accuracy in controlled environments, particularly indoors, where multipath propagation effects are strong. However, the primary drawback of fingerprinting is its dependency on exhaustive data collection. The process of creating a fingerprint database requires extensive on-site measurements, which can be labor-intensive and impractical for large or dynamic environments. Moreover, fingerprint databases must be updated periodically to account for environmental changes, further adding to the maintenance burden (Fan & Sun (2024)).

Another critical limitation of fingerprinting is the cost of hardware. High-precision fingerprinting requires specialized measurement devices such as software-defined radios (SDRs) or calibrated spectrum analyzers, which can be expensive. While commodity smartphones or Wi-Fi access points can sometimes be used, their accuracy and repeatability may be lower, leading to inconsistent results. The need for deploying multiple receivers across a large area significantly increases deployment costs (Chang *et al.* (2017)).

Several enhancements have been proposed to alleviate the limitations of traditional fingerprinting, such as crowdsourcing (Ye & Wang (2018)), radio map interpolation (Khoo, Ng & Tan (2022)), and machine learning-based feature extraction (Junoh & Pyun (2024)). While these techniques improve scalability, they do not fully eliminate the challenges associated with large-scale deployment and hardware cost.

1.1.2 Triangulation

Triangulation method estimates a transmitter's position based on measurements from multiple receiver nodes (Osa *et al.* (2013)). This approach relies on either the angle of arrival (AoA) or the time of arrival (ToA) of the received signal. Given at least three receiver nodes, triangulation calculates the intersection points of multiple circles (for distance-based methods) or lines (for angle-based methods) to estimate the transmitter's coordinates. Figure 1.2 illustrates position estimation of the rogue access point relying on AoA determinations.

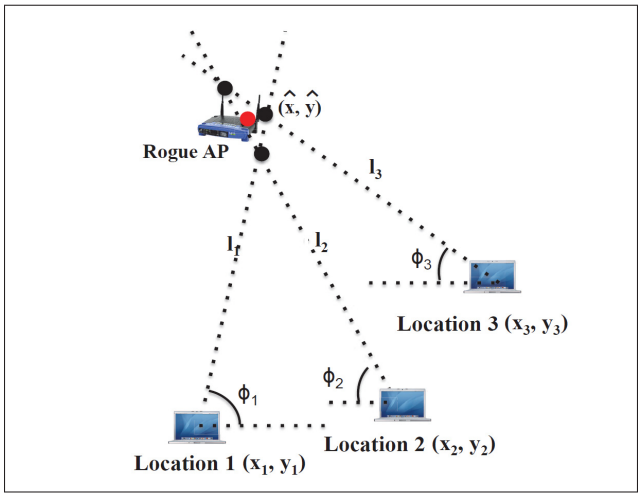

Figure 1.2 Localization of a rogue access point using triangulation
Taken from Zheng *et al.* (2014)
(Copyright © 2014, IEEE)

While triangulation methods work well in open-space environments with minimal obstructions, their accuracy degrades in complex environments due to multipath effects. Signal reflections, diffraction, and NLoS conditions can introduce errors in distance or angle estimates, leading to significant localization inaccuracies (Andersson, Lidström & Lindmark (2023)). Furthermore, the requirement for multiple synchronized receivers with precise position knowledge makes triangulation less practical for deployment in many real-world scenarios, especially where infrastructure is limited.

The cost of hardware required for triangulation is another important consideration. High-precision AoA and ToA measurements require specialized antenna arrays or synchronized receivers, which can be costly. SDRs and phased array antennas used for AoA-based localization are particularly expensive and require sophisticated calibration procedures. In contrast, low-cost alternatives, such as using mobile phones or Wi-Fi access points, can suffer from degraded localization accuracy due to hardware limitations and lack of synchronization (Chen, Lin, Kung, Lin & Gwon (2012)).

1.2 Deep Learning in Localization

Recent advancements in deep learning have provided new opportunities to overcome the limitations of traditional localization methods. By leveraging neural networks, deep learning models can learn complex, non-linear relationships between signal measurements and transmitter positions, leading to improved accuracy and robustness.

1.2.1 CNN-Based Models

CNNs have been extensively studied for localization tasks, particularly in the context of fingerprinting-based methods. CNNs are well-suited for learning spatial patterns from radio maps and RSS heatmaps, enabling improved generalization compared to traditional nearest-neighbor fingerprinting techniques (Jang & Hong (2018)).

Fig 1.3 illustrates the typical structure of a CNN, which consists of an input layer, multiple convolutional layers, pooling layers, a fully connected layer, and an output layer. The convolutional layer extracts features by performing inner product operations using multiple weighted convolution kernels. The pooling layer then downsamples the extracted features, reducing computational complexity and preventing overfitting. Finally, the fully connected layer processes the data for classification, utilizing dropout techniques to enhance model robustness before applying the SoftMax function to generate the final output.

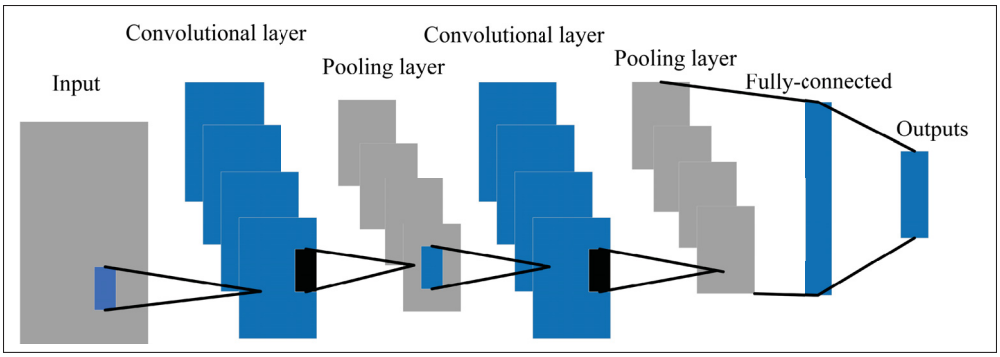

Figure 1.3 Structure of a conventional CNN
Taken from Zhu *et al.* (2023)

A significant limitation of CNN-based localization models is their reliance on full-grid measurements, requiring densely populated sensor deployments or extensive training datasets. Collecting such data is often impractical, particularly for large-scale environments where full radio maps are unavailable (Alzubaidi *et al.* (2021)).

1.2.2 Reinforcement Learning-Based Approaches

Reinforcement learning (RL) has been explored as a means of optimizing localization strategies, particularly in dynamic or resource-constrained environments (Li *et al.* (2020)). RL-based methods treat localization as a sequential decision-making problem, where an agent learns to move or adjust measurement locations to minimize localization error (Dou, Lu, Zhu & Bi (2024)).

Figure 1.4 showcases an architecture for RL-based wireless localization method. The agent operates in an environment where its state consists of its location and RSS measurement. It selects actions from a set of nine possible movements, including staying in place and moving in eight cardinal and diagonal directions. The reward function provides positive reinforcement for correct actions, typically based on geographical distance to a target.

Despite their potential, RL-based localization techniques are computationally expensive. Training an RL model requires significant computational resources, and real-time execution may demand

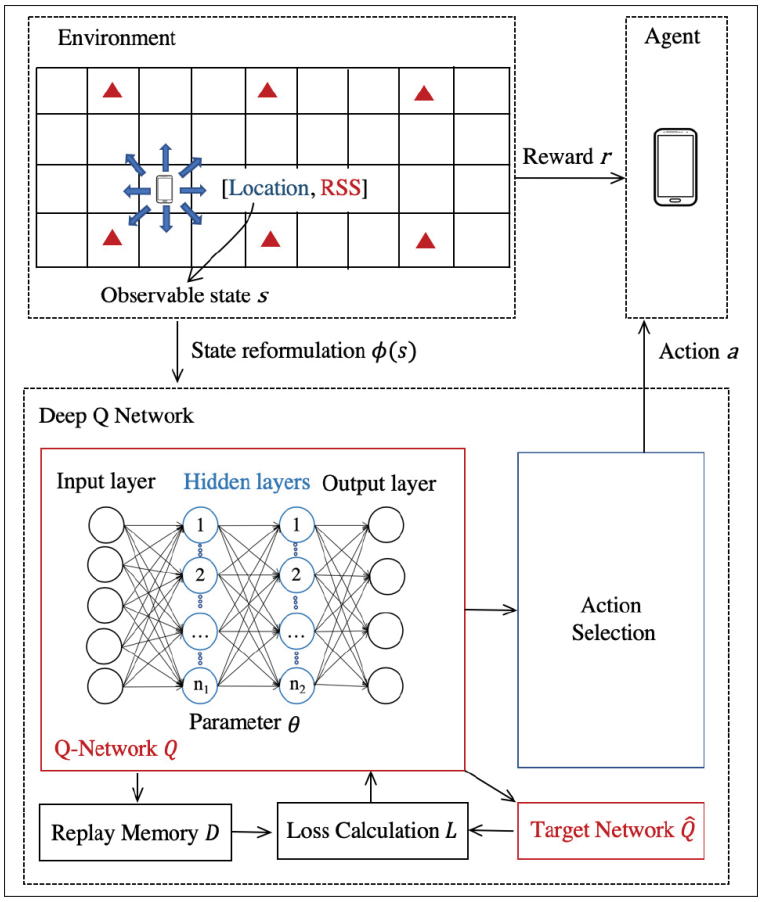

Figure 1.4 A localization method based on reinforcement learning
Taken from Li *et al.* (2020)
(Copyright © 2020, IEEE)

specialized hardware (Alagha, Mizouni, Singh, Bentahar & Otrok (2025)). Additionally, RL models often require extensive exploration of the environment, making their application limited in restricted environments.

1.2.3 ResNet for Localization

Residual networks (ResNets) have emerged as a promising alternative for localization tasks, balancing model depth with computational efficiency. ResNet architectures employ skip

connections to mitigate the vanishing gradient problem, allowing for the training of deep networks without excessive parameter growth (He, Zhang, Ren & Sun (2016)).

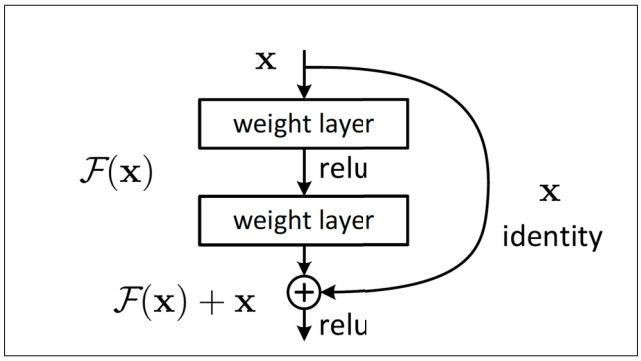

Figure 1.5 Building block of a ResNet
Taken from He *et al.* (2016)
(Copyright © 2016, IEEE)

Figure 1.5 shows the building block of a residual learning scheme. Here x and y are the input and output vectors and the function F(x) represents the residual mapping to be learned.

Unlike full-grid CNN approaches, ResNets can be adapted to work with sparse input data, making them more suitable for real-world applications (Guo, Sun, Jian & Zhang (2018)). Furthermore, ResNet models require less computational hardware compared to conventional CNN-based learning models, making them a more effective solution for large-scale deployments (Shafiq & Gu (2022)).

1.3 Research Gap

Traditional localization methods require dense measurements and precise infrastructure, limiting their feasibility in resource-constrained environments. Fingerprinting is labor-intensive and costly due to its reliance on extensive data collection, while triangulation depends on synchronized receivers and high-precision hardware. These methods also struggle with the inconsistent data from low-cost commercial off-the-shelf (COTS) equipment, highlighting the need for more adaptable approaches that perform reliably with sparse measurements. Furthermore, most deep

learning-based localization models necessitate measurement data from various points across the map to generalize effectively. Their performance deteriorates when applied to data collected along a single path, as they fail to capture spatial variations across the broader environment. This heavy dependence on exhaustive data collection limits their practicality, particularly in large-scale or restricted-access areas where comprehensive measurements are infeasible. In summary, current localization methods often trade practicality for performance: they assume big measurement data and big computing power, which is a gap when considering real-world deployment constraints.

CHAPTER 2

A RESIDUAL NEURAL NETWORK APPROACH TO TRANSMITTER LOCALIZATION

Arash Ahmadi[1] , Abhiroop Bhattacharya[1] , Fabrice Vaussenat[1] , Sylvain G. Cloutier[1] , Richard Al Hadi[1]

[1] Département de Génie Électrique, École de Technologie Supérieure,
1100 Notre-Dame Ouest, Montréal, Québec, Canada H3C 1K3

Article accepted by the journal "IEEE Transactions on Microwave Theory and Techniques" in November 2025.

Abstract: This paper presents a method for locating a wireless signal source using signal strength measurements taken along the border of a 256×256-m^2 area. The method leverages a deep Residual Neural Network (ResNet) to predict the location of the transmitter within the area of interest. This approach reduces data collection and computational overhead associated with traditional localization methods. The method is validated through simulated data as well as measurements at 2.7 GHz, with an average error of 7.23 m and a standard deviation of 3.32 m. This work addresses the need for scalable and low-cost transmitter localization methods, particularly in environments where conventional approaches are hindered by obstacles or require extensive data collection.

Keywords: Radio frequency, propagation map, deep learning, ResNet, convolutional neural network, CNN, signal localization.

2.1 Introduction

Wireless transmitter localization is essential for planning and managing communication networks as well as detecting rogue transmitters that interfere with network operation (Wang, Zheng, Chen & Yang (2017)). However, locating transmitters in dense urban environments remains a challenging task due to multipath, shadowing, and the presence of obstacles.

Localization methods can be divided into several categories: geometric approaches such as triangulation and multilateration, model-based propagation algorithms, fingerprinting, and machine learning (ML)-based data-driven techniques.

In fingerprinting, a detailed map of signal strengths is created at known points within the area of interest, and later measurements are matched against this "radio map" to estimate the transmitter's position (Nurminen *et al.* (2017)). While fingerprinting can capture complex propagation effects, it requires extensive data collection with laborious on-site measurements, which can be impractical for large or dynamic environments. In contrast, model-based algorithms convert measured signal strength into distance information by fitting to a statistical or physical path-loss model. Source positions are then calculated using distances between the transmitter and measurement points with known coordinates. Properties such as Received Signal Strength Indicator (RSSI), Time of Arrival (ToA), and Angle of Arrival (AoA) are commonly exploited in these probabilistic models (Osa *et al.* (2013)). However, their performance degrades significantly in cluttered or non-line-of-sight (NLoS) environments, and they add computational overhead in complex scenarios. A computationally inexpensive alternative is triangulation, which estimates the transmitter's position from angles and distances across multiple receiver points (Elsanhoury *et al.* (2022)).

Research in recent years has extended these classical methods. For example, high-resolution AoA estimation with hybrid arrays has improved the angular precision of direction-finding (Chuang, Wu & Liu (2015)), while hybrid approaches have been proposed that jointly exploit Time Difference of Arrival (TDoA), Frequency Difference of Arrival (FDoA), and Phase Difference of Arrival (PDoA) measurements to enhance robustness (Zhang, Wen, Zhao & Xu

(2024); He & Dong (2017)). RSS-based methods have also been shown to be improved with weighted least squares parameters in mixed line-of-sight (LoS) and NLoS conditions (Sun, Yang, Wang & Chen (2021)).

Parallel to these advances, machine learning has emerged as a powerful tool for transmitter localization. Early works trained neural networks to learn the nonlinear mapping from RSS measurements to positions combined with probabilistic models (Zhang, Liu, Zhang, Zhang & Gu (2016)). Recently, deep learning has led to sophisticated frameworks such as DeepTxFinder, which uses a convolutional neural network (CNN) to jointly predict the number and locations of multiple transmitters from crowdsourced spectrum sensing data (Zubow, Bayhan, Gawłowicz & Dressler (2020a)). Similarly, DeepMTL employs a two-stage pipeline combining a U-Net encoder–decoder with a detector based on You Only Look Once (YOLO) algorithm to improve accuracy and generalization (Zhan, Ghaderibaneh, Sahu & Gupta (2022)). Other architectures such as calibrated U-Nets have been explored for robust localization under sparse sensors or model mismatch conditions (Mitchell, Patwari, Bhaskara & Kasera (2023a)). Encoder–decoder CNNs have also been proposed for fine-grained likelihood maps that generalize across environments (Levie, Yapar, Kutyniok & Caire (2021)).

Meanwhile, researchers have applied ML more broadly to problems in microwave engineering, including dielectric property estimation (Luo *et al.* (2024)), improved spatial resolution in near-field probing (Cho & Simsek (2024)), RSSI-AoA estimation for indoor positioning (Yen, Ou Yang & Tsai (2022)), radar classification with model-based data augmentation (Rojhani, Passafiume, Sadeghibakhi, Collodi & Cidronali (2023)), and biomedical applications (Lu, Xiao, Pang, Liu & Lu (2022)).

This paper builds upon the authors' prior work in CNN-based propagation modeling (Ahmadi, Bhattacharya, Gratuze, Cloutier & Hadi (2025a)), which demonstrated how boundary measurements can be used to infer path loss without prior transmitter knowledge. Inspired by that framework, here we extend the approach to the more complex task of transmitter localization using a ResNet-based architecture. The proposed model leverages deep residual connections to efficiently learn

from boundary-only measurements and predict transmitter coordinates. Unlike fingerprinting or model-based methods, this approach does not require dense in-area sampling or a pre-surveyed map. Instead, it relies solely on signal strength measurements collected along the accessible borders of an area, thereby reducing data collection overhead while maintaining accuracy in challenging environments. The proposed method is particularly suitable for applications such as detecting rogue transmitters that interfere with network operation, locating transmitters during emergency situations like earthquakes or floods when access is restricted, identifying transmitters inside an area where the internal layout is unknown, and supporting law enforcement agencies in tracking illegal radio transmissions. These scenarios benefit from the method's ability to operate under limited prior knowledge and constrained measurement conditions.

The rest of the paper is organized as follows: Section 2.2 describes the proposed methodology in detail, the model and dataset used based on the signal propagation and localization challenges. Section 2.3 outlines the training procedure and compares the resulting outcomes across the simulations. Section 2.4 presents the results and presents insights of the proposed method. Finally, Section 2.5 discusses advantages, limitations, and future directions of this study.

2.2 Methodology

In an unobstructed, open space with no reflectors or barriers, the received power of a signal from a wireless transmitter on a specific frequency is determined entirely by the distance between the transmitter and client device. For example, if the transmitter is at position X, and the receiver is at position Y, the distance will be $l = |X - Y|$. The received signal power in this scenario, denoted as P_R, can be expressed as $P_R = f(l)$. In this straightforward scenario, the goal of a localization system is to model a function that maps the received signal power back to the user's position.

However, the situation becomes significantly more complicated when multiple objects in the environment reflect or obstruct the signal. If the shape, size, and positions of these objects are represented as a set of hyperparameters, θ, the received signal power at the client device, denoted

as P'_R, can be modeled as $P'_R = f'(l;\theta)$. This introduces a high level of complexity because the signal now depends on numerous factors such as reflection, refraction, and diffraction.

In localization tasks, no direct knowledge of θ is available, which makes it even more difficult to determine the signal-mapping function corresponding to f'. The key insight is to leverage neural networks to model this complex signal-mapping function as a black box. Recent advances in deep learning favor using neural network representations over traditional hand-crafted models, often leading to better performance. This approach enables the signal's environmental effects to be implicitly captured by incorporating them into the network's parameters, which are learned from observed ground truth data.

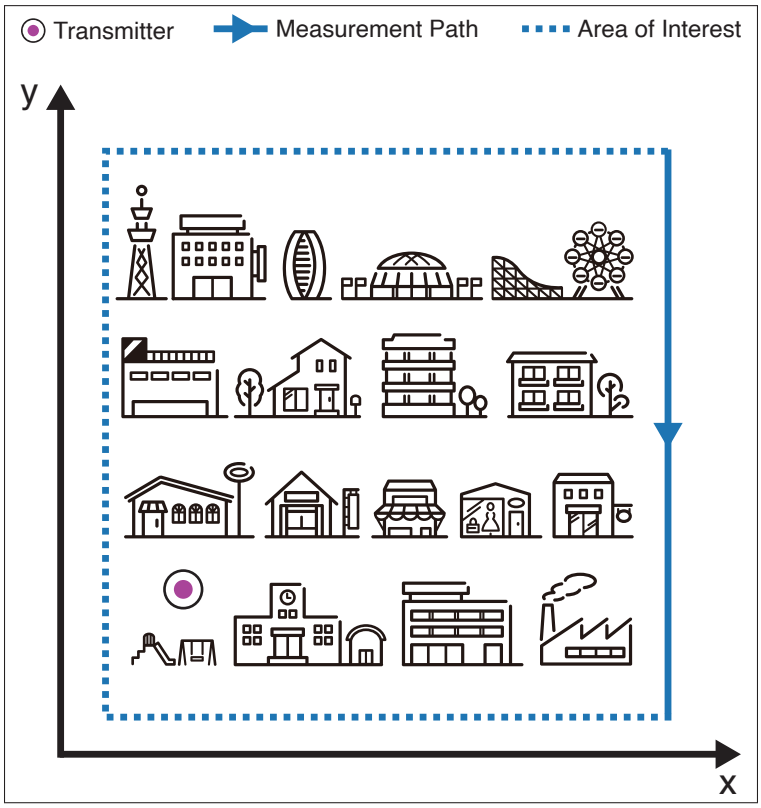

Figure 2.1 Task overview: the transmitter is located inside the area of interest, while signal strength measurements are collected along the accessible border, following a straight path

In this study, the localization task is defined over a two-dimensional area of 256×256-m^2. The boundary measurements inherently include contributions from multi-path (e.g., reflections from nearby buildings) and out-of-domain. Our model treats such effects as part of the observed boundary field. The measurements is not collected throughout the area but are instead limited to its borders, such as streets or accessible perimeters, along which signal strength is recorded at regular intervals. An overview of the localization task is provided in Fig. 2.1, where the measurement path, direction of data collection, area of interest, and the transmitter to be localized are indicated. Under such constraints, traditional localization techniques including triangulation, fingerprinting, and other centroid-based methods are not applicable, as these approaches typically rely on scattered measurements across the interior of the region. As a result, a different approach is required that can infer transmitter locations using only signal strength values collected along the border of the area, without access to internal measurements or prior knowledge of the environment's layout.

2.2.1 Description of ResNet and its benefits

Residual Networks (ResNet) were introduced as a solution to the degradation problem often encountered when training very deep neural networks (He *et al.* (2016)). ResNet introduces shortcut connections that allow the network to bypass one or more layers, enabling it to learn residual functions rather than directly fitting the data to complex mappings. A ResNet consists of residual blocks and the output of each of these blocks is defined as:

$$y = F(x, W_i) + W_s x \tag{2.1}$$

where x is the input to the residual block. The residual function is represented by $F(x, W_i)$. The term x is added via an identity connection. Sometimes, a projection layer W_s can be used to match the dimension. This residual learning framework significantly enhances optimization, as the network focuses on learning the difference (or residual) between the output and input. ResNet's architecture makes it particularly well-suited for applications that require deep representations while avoiding issues like vanishing gradients. Additionally, its ability to scale to hundreds or

even thousands of layers without performance degradation makes it a powerful tool for complex pattern recognition tasks. ResNet architecture is highly suitable for sequential data like signal measurements (Chen, Zhao, Yang & Dai (2023)).

Given these properties, ResNet can be used in wireless communication applications where sparse sequential data is present, such as estimating the location of transmitters based on limited signal strength measurements (Cao, Lv, Lin, Huang & Lin (2020)). The network's capacity for learning detailed spatial relationships from limited inputs enables localization even in environments with multipath effects and propagation uncertainties.

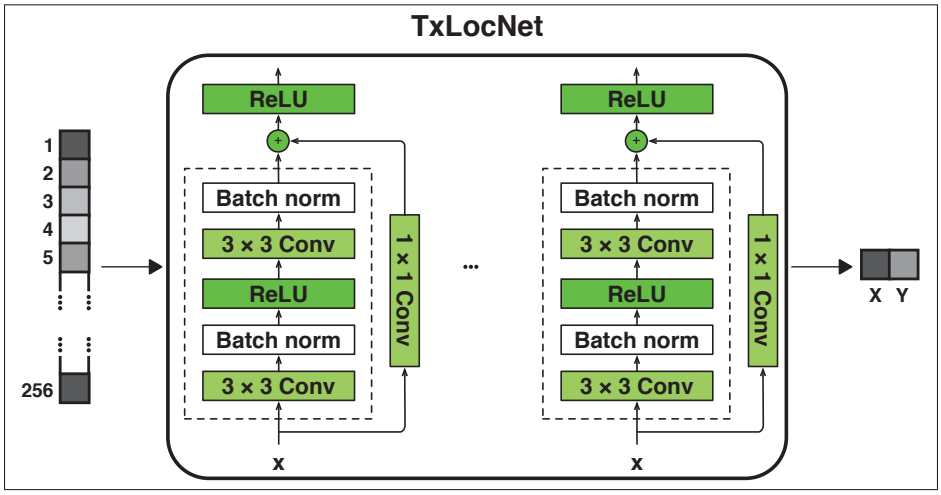

Figure 2.2 TxLocNet overview: border measurements as input vector, ResNet-based inference model, predicted transmitter location coordinates as output

Based on these findings, a ResNet-based model is proposed here for locating a wireless transmitter, called TxLocNet. The proposed model's overview is shown in Fig. 2.2. A vector containing path loss data from the border of the layout is used as input for TxLocNet. This vector can be acquired by running a simulation or conducting a measurement. The output is a set of two values that predict the Tx location along the x- and y-axis, respectively. As shown in Fig. 2.2, each module of the model has 2 convolution layers with a 3×3 kernel followed by a batch normalization layer to stabilize the training and improve convergence. The model uses skip connections with a 1×1

convolution layer so that the output can be captured by adding the previous module to the output of the current module (Zhang, Lipton, Li & Smola (2023)). The proposed architecture has 4 such aforementioned modules. The input vector consists of 256 measurements of the shape 256×1. This vector is preprocessed by expanding along the horizontal dimension to create a two dimension vector. This enables us to use it with a 3×3 kernel. Since this model uses spatial symmetry for estimating the location of the transmitter, the model uses a 2D convolution kernel. This is aligned with recent work in literature (Levie *et al.* (2021); Ahmadi *et al.* (2025a)).

2.2.2 RadioMapSeer Dataset

This work is based on the publicly available RadioMapSeer dataset, consisting of 700 urban radio maps, each featuring 80 distinct transmitter locations with corresponding radio maps generated using the Dominant Propagation Model (DPM) method (Yapar *et al.* (2022)). DPM considers the dominant path between transmitter and receiver (every pixel) and predicts the path loss along that path. The computation of the path loss P_L is based on the following equation (Wahl & Wolfle (2006)):

$$P_L = 20\log(\frac{4\pi}{\lambda}) + 10p\log(l) + \Sigma_{i=1}^{n} f(\phi, i) + \Sigma_{j=1}^{m} t_j - \Omega \tag{2.2}$$

Here, P_L in decibels depends on the path length l, wavelength λ, and waveguiding factor Ω, which represents the influence of nearby structures on wave propagation. Each interaction i affects the loss according to the angle ϕ of direction change; losses diminish as the wave diffuses after each interaction. For every wall encountered, t_j denotes the transmission loss of wall j, accounting for indoor settings where wall penetration impacts signal strength. The factor p adjusts the calculation for Line-of-Sight (LoS) or Non-Line-of-Sight (NLoS) conditions.

The RadioMapSeer dataset is based on urban layouts extracted from OpenStreetMap, encompassing multiple global cities. In Yapar *et al.* (2022), the simulations were carried out using WinProp software (Hoppe, Wolfle & Jakobus (2017)), producing densely sampled radio maps on a 2D

grid. In the dataset, the radio map for each layout is available as a gray-scale image with a resolution of 256×256 pixels, corresponding to an area of 256×256 m^2. The transmitter, receiver, and building heights are fixed at 1.5 m, 1.5 m, and 25 m, respectively.

The path loss P_L values from the simulated radio maps are then converted into gray-scale pixel values ranging from 0 to 255 using the following formula (Levie *et al.* (2021)):

$$\mathrm{GS} = \frac{P_L - P_{L,\mathrm{trnc}}}{M_1 - P_{L,\mathrm{trnc}}} \times 255 \tag{2.3}$$

where P_L is in dB. In this equation, M_1 represents the maximum P_L across all radio maps which is set to -47.84 dB. $P_{L,trnc}$ denotes the truncation threshold for P_L and is set to -147 dB. In this conversion, GS = 0 represents values below the analytic noise floor, while GS = 255 corresponds to the maximum gain at the transmitter. Intermediate gray-scale values are used to encode the range of path loss values, effectively providing a visual representation of the radio maps. In cases where building are present or measurements are missing, the data point as considered as GS = 0.

Although DPM is a simplified propagation approach, it accounts for the primary signal path, which may involve reflection, diffraction, and transmission effects (Wahl & Wolfle (2006)). While it does not capture the entire multipath profile, it identifies the most influential propagation mechanism between transmitter and receiver for each location. Therefore, the resulting dataset includes signal characteristics shaped by major environmental interactions, allowing the model to learn spatial relationships that reflect real-world propagation behavior, especially in complex urban settings.

To represent border measurements, the original dataset is modified by considering only the rightmost border of each image as shown in Fig. 2.3.

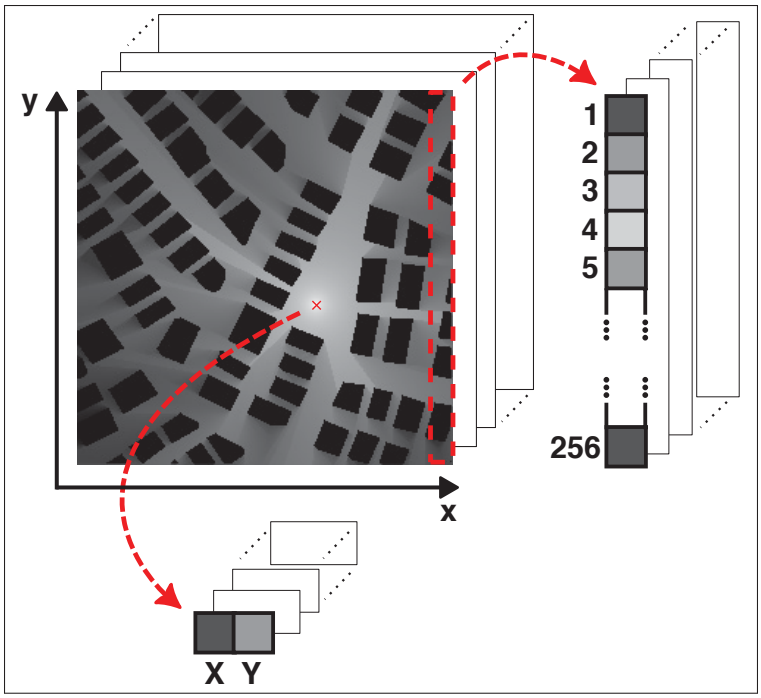

Figure 2.3 Dataset: Path loss maps from RadioMapSeer; boundary vectors from path loss maps (input for TxLocNet), corresponding Tx locations (target for TxLocNet)

2.3 Model Training

2.3.1 Training Procedure

As mentioned in the previous section, the RadioMapSeer dataset includes radio maps simulated from 700 urban layouts, each with 80 different transmitter locations, resulting in 56,000 samples (Yapar *et al.* (2022)). Training the model using such a large and diverse dataset approach enables the model to learn generalized spatial features and infer transmitter locations without requiring prior knowledge of specific building layouts. The dataset is shuffled and broken into 3 parts: 39,200 samples (70%) for training set, 8,400 samples (15%) for validation set, and 8,400 samples (15%) for test set. The model is trained on the dataset using a uniform random permutation sampler by PyTorch which draws from the training data with equal probability,

without replacement. The training also uses the Adam optimizer (Kingma & Ba (2015)) to minimize the loss function, which measures the difference between predicted and actual signal strength maps. The mean squared error (MSE) is used as the loss function for the training as described in Eq. 2.4.

$$\text{MSE} = \frac{1}{n}\sum_{i=1}^{n}(y_i - \hat{y}_i)^2 \tag{2.4}$$

where n is the number of samples in the batch, y_i is the ground truth (target location), and $\hat{y}_i$ is the predicted location from TxLocNet.

After the training phase, the model will be evaluated in its ability to predict transmitter locations based on border measurements regardless of the layout.

2.3.2 Performance on Test Data

For evaluation purposes, the test set (a portion of dataset that is "unseen" by the model during the training) is fed to the model. The error is calculated using the Euclidean distance between the actual location (from the dataset) and predicted location (model's output). It is noteworthy to add that the number of layers are chosen based on availability of pre-trained weights. Table 2.1 presents a comparison of the proposed model architecture with other state of the art deep learning architectures. To ensure a fair comparison, all deep learning architectures listed in the table were trained on the same dataset (RadioMapSeer). Each neural network was adapted to match the task-specific input and output dimensions: the input vector of size 256×1, representing the rightmost border of each signal strength map, and the output vector of size 1×2, corresponding to the predicted transmitter's x and y coordinates. Necessary architectural adjustments (e.g., modifying input layers and final fully connected layers) were made to accommodate these dimensions while preserving the core design of each model.

Although the vanilla CNN and MobileNetv2 architectures have a lower number of parameters, it is observed that the average error is very high which motivated the use of more complex model

architectures. The WideResNet and ResNeXt architectures have a much larger number of model parameters which makes them computationally expensive and difficult to deploy in terms of cost and energy requirements (Ning, Vandersteegen, Van Beeck, Goedemé & Vandewalle (2024)). The ResNet architecture provides a good balance between the number of model parameters and the model performance. It is empirically observed that the ResNet model architecture with 50 layers gives the optimum trade off between the model performance and model parameters. Most importantly, it gives the lowest average error with the lowest standard deviation compared to the other tested models.

Table 2.1 Comparison of TxLocNet performance with different deep learning architectures

Neural Network	**No. of Layers**	**No. of Params**	**Average Error (m)**	**Variance of Error (m^2)**	**Standard Deviation of Error (m)**	**Max. Error of the Best 25% (m)**	**Max. Error of the Best 50% (m)**	**Max. Error of the Best 75% (m)**
CNN Lecun, Bottou, Bengio & Haffner (1998)	4	496,682	42.63	162.46	49.25	10.63	24.24	55.32
MobileNetV2 Sandler, Howard, Zhu, Zhmoginov & Chen (2018)	53	2,225,858	31.29	155.72	37.61	9.55	18.49	45.49
ResNet He *et al.* (2016) **(used in TxLocNet)**	18	11,171,266	25.94	150.37	29.97	6.47	14.75	33.67
	34	21,279,426	13.74	131.24	15.87	3.43	7.81	17.82
	50	**23,505,858**	**9.34**	**116.45**	**10.79**	**2.33**	**5.31**	**12.12**
	101	42,497,986	12.87	118.41	14.87	3.21	7.32	16.70
	152	58,141,634	11.52	122.87	13.31	2.87	6.55	14.95
WideResNet Zagoruyko & Komodakis (2016)	50	66,832,066	12.03	120.36	13.90	3.00	6.84	15.61
	101	124,835,522	10.89	117.53	12.58	2.72	6.19	14.13
ResNeXt Xie, Girshick, Dollár, Tu & He (2017)	50	22,977,730	11.82	119.32	13.66	2.95	6.72	15.34
	101	86,740,162	10.28	118.47	11.88	2.56	5.84	13.34

The training time for TxLocNet with a 50-layer ResNet architecture with was 5 hours and 32 minutes on a server with Intel Xeon CPU (1 core), 1 GB of RAM, and a Nvidia T4 GPU (with 16 GB of VRAM). After the model is trained, the inference runtime is about 0.40 seconds on a conventional laptop (without dedicated GPU).

The average error of the trained TxLocNet is 9.34 m and as evident in Fig. 2.4, the error is less than 20 m for the majority (88%) of the test set. It is important to note, the model's error cannot go below 1 m because each pixel in the dataset used for training represents 1 m^2.

A repository containing the TxLocNet dataset, model, training and test scripts are uploaded to Ahmadi, Bhattacharya, Vaussenat, Cloutier & Al Hadi (2025b).

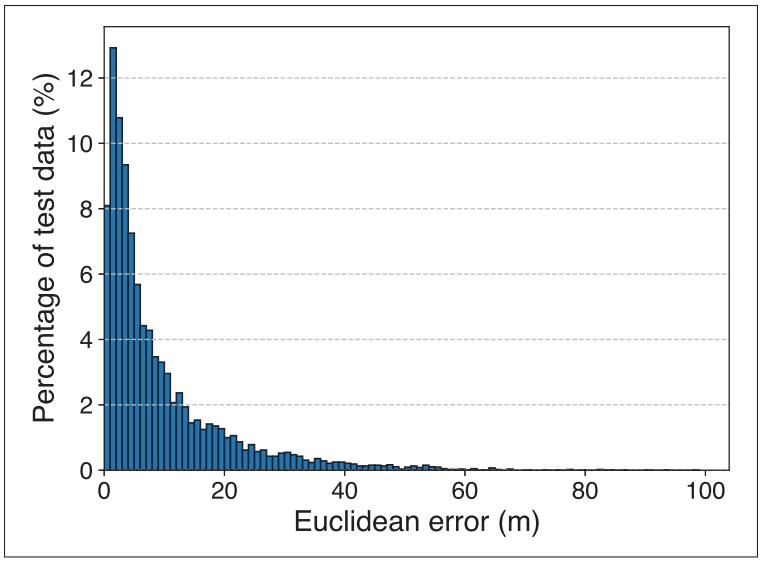

Figure 2.4 The percentage histogram of TxLocNet localization error on test dataset of 8,412 images

2.3.3 Remedy for outliers scenarios

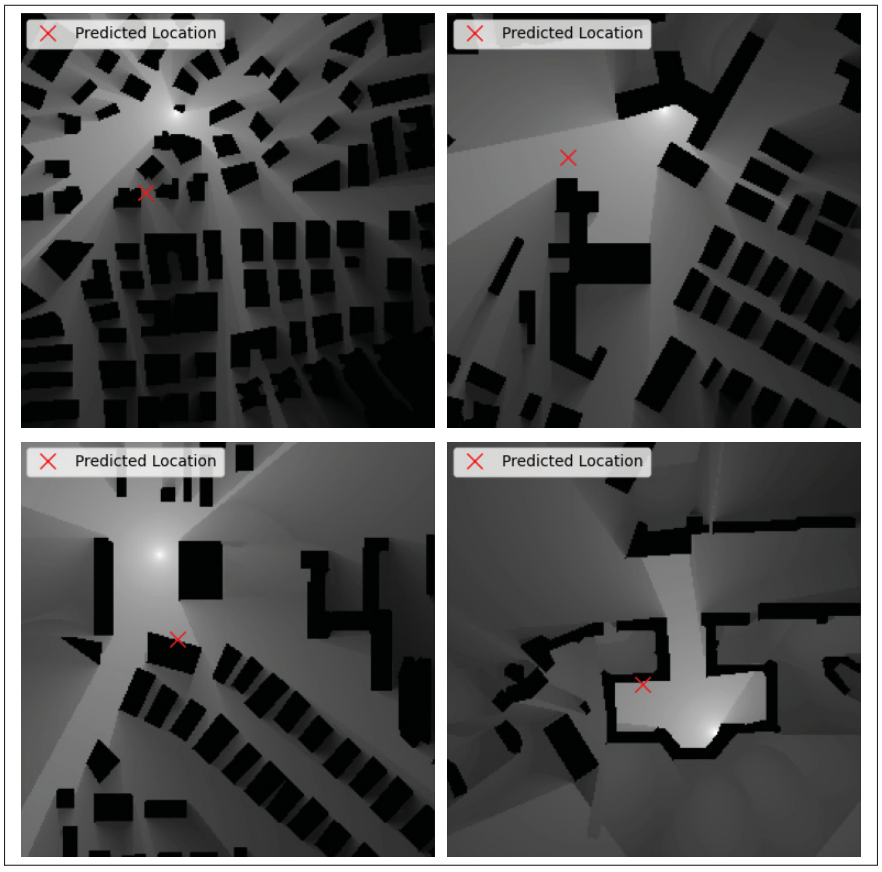

Figure 2.5 Scenarios where TxLocNet predicts the Tx location with high errors

Looking at the high variance in the model error (116.45 m^2), some outliers can be observed. These outliers are believed to occur in non-ideal situations where the transmitter is surrounded by walls or the measurement path is blocked by walls, as shown in Fig. 2.5. To prove this hypothesis, an index called "Confidence" introduced to help better understand when the model has reliable output. The numerator of this index is defined as the sum of the path loss from the border of the area of interest. In order to calculate the denominator, an empty area (free space) is considered and a Tx is placed at the predicted location and the path loss map is generated using the Free Space Path Loss (FSPL) formula (Rappaport (2001)). The denominator of the

index is defined as the sum of the path loss data from the border of the free space area. The Confidence index formula can be expressed as follows:

$$\text{Confidence index} = \frac{\sum_{i=1}^{n} P_{L,i}}{\sum_{i=1}^{n} P_{\text{FSPL},i}} \tag{2.5}$$

where $P_{L,i}$ is the path loss form the border of the area of interest and $P_{\text{FSPL,i}}$ is the path loss from the border of the area, generated using the FSPL formula. The confidence index is always bounded between 0 and 1 by definition, with higher values indicating greater reliability of the prediction. It is designed to be used as a normalized measure of the model's certainty.

Fig. 2.6 shows a scatter plot of TxLocNet error along x- and y-axis versus the Confidence index. It is apparent form the scatter plot that in scenarios where the Confidence index is low, the error becomes higher. Table 2.2 shows the performance of TxLocNet when considering subsets of the test set based on increasing confidence index thresholds. As the confidence threshold increases, the average, maximum, and variance of localization error consistently decrease, indicating that the confidence index is a reliable predictor of estimation accuracy. It is observed that when the confidence index exceeds 0.4, the model achieves a significant improvement in localization accuracy, reducing the average error from 9.34 m (full test set) to 5.44 m and the error variance from 116.46 m^2 to 39.19 m^2. This indicates that a threshold of 0.4 serves as a practical cutoff for reliable predictions.

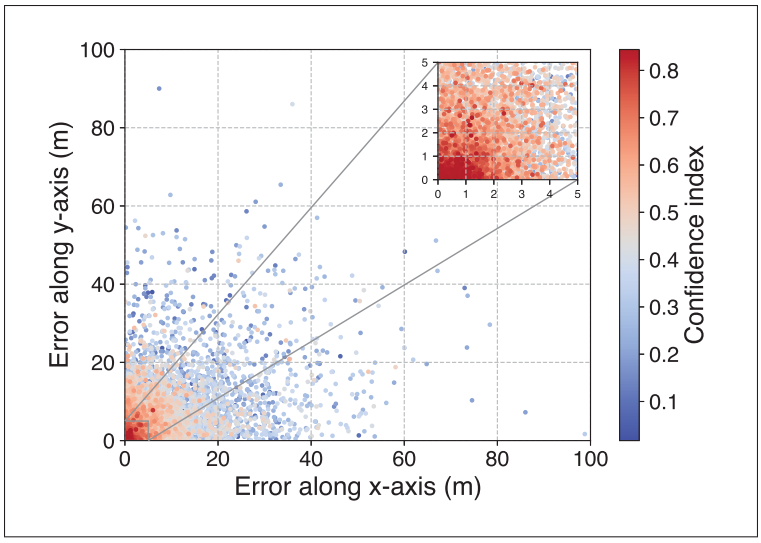

Figure 2.6 Scatter plot of TxLocNet error on the test data along x- and y-axis. The color gradient showcase the amount of confidence index

Table 2.2 Localization performance of TxLocNet across different confidence-index thresholds

Test Set Subset	**Average Error (m)**	**Variance of Error (m)**	**Standard Deviation of Error (m^2)**
Conf. > 0.8	0.78	3.68	0.25
Conf. > 0.7	1.31	9.83	1.09
Conf. > 0.6	2.08	18.93	3.41
Conf. > 0.5	3.51	55.17	15.63
Conf. > 0.4	**5.44**	**64.13**	**39.19**
Conf. > 0.3	7.55	98.79	79.02
Conf. > 0.2	8.79	98.79	104.36
Conf. > 0.1	9.27	98.79	115.08
Complete	9.34	98.79	116.46

However, if the Confidence index is below 0.4 then the measurement of the last vector might not be sufficient to correctly predict the transmitter location. In this scenario, it is prudent to take additional measurements. The observer should make another measurements with higher Confidence index. This analysis has been performed on a sample scenario with obstructed

transmitter on Fig. 2.7. The top portion of the figure displays the path loss map with the measurement path highlighted by a red dashed rectangle. The plot in the lower portion of the figure shows that after changing the measurement path by 30 m, the Euclidean error decreases with an increase in the Confidence index. Thus, it is suggested that the limitations of the proposed method can be reduced by additional measurements. As evident in Fig. 2.7, it is noteworthy to mention that model's error along y-axis is lower compared to the error along x-axis which mainly contributes to the Euclidean error.

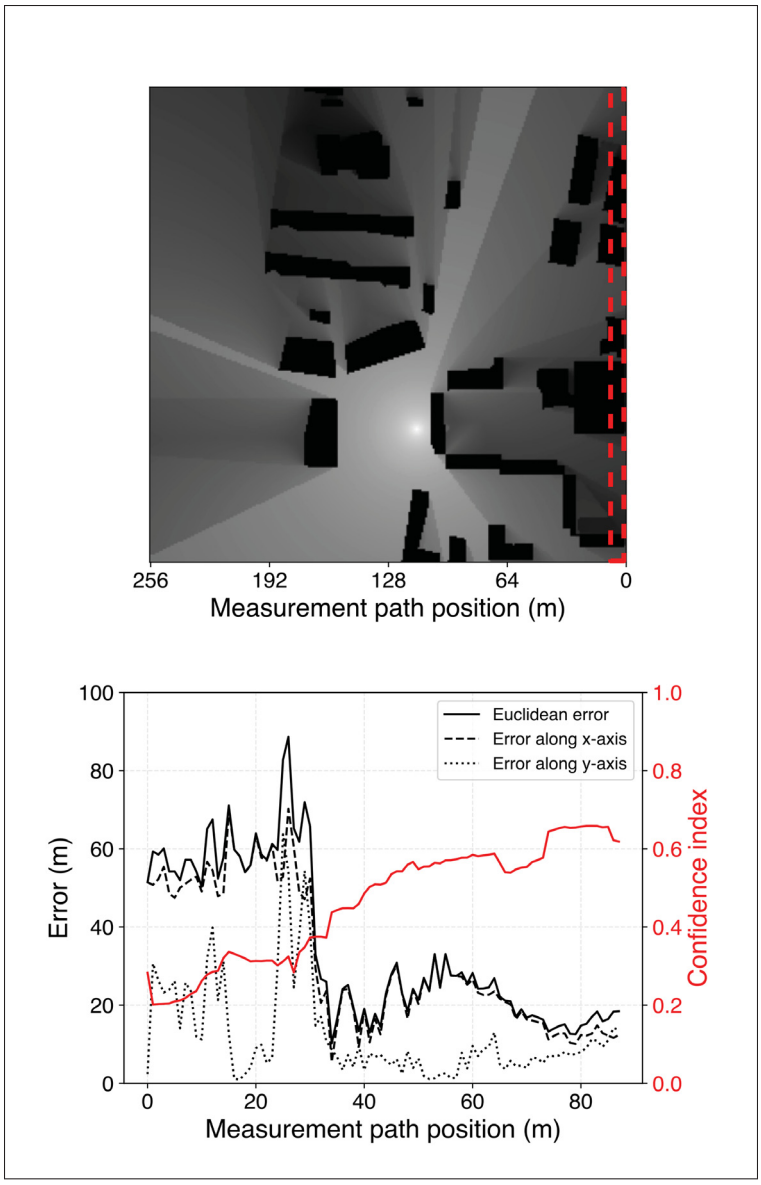

Figure 2.7 Top: path loss map of a scenario where the signal from the transmitter is obstructed by obstacles; bottom: TxLocNet error and confidence index vs measurement path position

2.4 Measurements

2.4.1 Setup for Measurements

To validate the proposed approach in real-world settings, the measurements are performed in outdoor environments with known transmitter locations. For this purpose base stations are considered in 4 locations in urban areas (Montréal, Québec, Canada) as shown in Fig. 2.8 and conducted 12 tests to determine the transmitter locations. For each area, the measurements path is shown in full line while the area of interest is surrounded by a dashed line. An Android smartphone (Samsung Galaxy S23 FE) is used as a measurement device and data collection is preformed using G-NetTrack Pro application. Smartphone antenna measurements indicate that, although not perfectly isotropic, the radiation characteristics of handset antennas in the mid-band frequencies are generally close to omnidirectional in the azimuth plane (Horansky, Coder & Ladbury (2019)). Using this handset for signal strength measurement offers a cost-effective and energy-efficient alternative to traditional dedicated hardware, which is often expensive and power-intensive. Equipped with Snapdragon X70 Modem, the handset provides reliable signal metrics like Reference Signal Received Power (RSRP). The reporting range of RSRP is defined from -140 dBm to -44 dBm (ETSI (2020)), which is sufficient for lightweight measurement scenarios where high accuracy is not required.

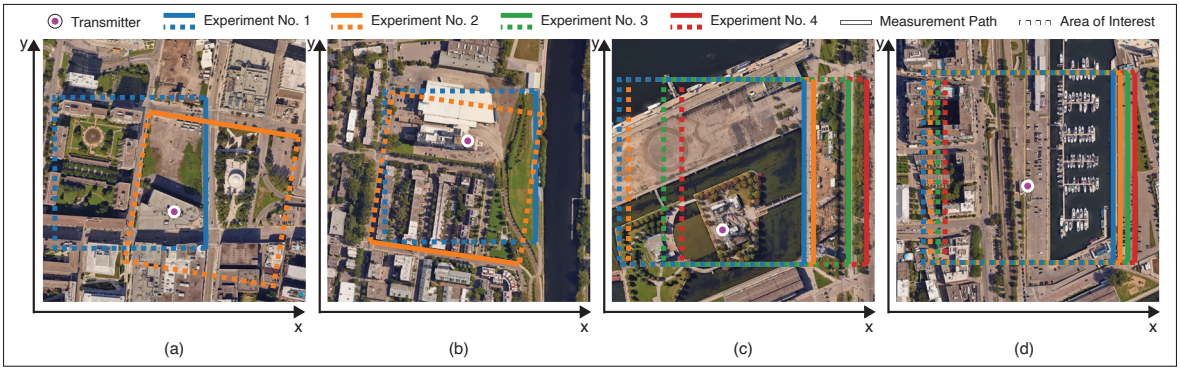

Figure 2.8 Aerial views of the measurement locations

2.4.2 Data Collection Process

A 256-m by 256-m area is considered with the base station located within. Along one border of the area, 256 received signal strength measurements were collected at 1-meter intervals using a standard communication handset. The measured data is filtered so that it only includes data from a single base station operating on LTE band number 7 with downlink frequency of 2680 MHz using 3350 as EARFCN (E-UTRA Absolute Radio Frequency Channel Number) (ETSI (2020)). It is noteworthy that RSRP is measured in dBm, but as mentioned in Section 2.2, model is trained on gray-scale (GS from Eq. 2.3) which is derived from path loss in dB. To ensure relevance of the collected data, it is necessary to subtract the transmitter's signal power, also measured in dBm, from the RSRP to derive path loss in dB. The power output of base stations varies with their size; however, microcells, which are commonly deployed in urban environments, typically operate with a power output of approximately 30 dBm.

2.4.3 Results

The collected data was then fed into the trained ResNet model to predict the transmitter's location. The Table 2.3 compares the model's predictions against the actual transmitter positions, achieving an average localization error of 7.23 m with a standard deviation of 3.32 m. These results closely matched the test set outcomes, demonstrating the model's applicability to practical scenarios. The location (a) refers to the university campus which has a high density of buildings resulting in reflection, attenuation and obstruction of the transmitter signal. This results in a higher average error of 9 m. While the (b) environment is situated on a canal which has a low density of buildings leading to a low average error of 3.5 m. The environments named (c) and (d) are situated in a port area which has structures on the banks leading to variance in model accuracy depending on the location of the transmitter and receiver.

Furthermore, the results from measurements at locations (c) and (d) indicate that the model exhibits robustness to small displacements of the transmitter, with average Euclidean localization errors of 8.52 m and 7.06 m, respectively. In both cases, the measurement paths were arranged

in parallel with fixed spacing, effectively simulating changes in transmitter position. This setup demonstrates the model's ability to maintain accuracy under slight variations in transmitter location.

Table 2.3 TxLocNet accuracy using measurements at various locations

Location	No.	Euclidean Error (m)	Confidence Index
(a)	1	7.55	0.50
	2	10.41	0.48
(b)	1	3.79	0.55
	2	2.62	0.56
(c)	1	6.73	0.54
	2	13.79	0.47
	3	6.85	0.52
	4	6.72	0.51
(d)	1	8.56	0.59
	2	2.86	0.63
	3	6.08	0.58
	4	10.74	0.57

2.5 Discussion

2.5.1 Comparison with State-of-the-Art

State-of-the-art (SotA) methods for transmitter localization have been demonstrated through deep learning techniques, each offering unique advantages and trade-offs. The proposed method, TxLocNet, distinguishes itself by using only border measurements and leveraging a ResNet-based CNN to predict transmitter coordinates. To contextualize TxLocNet's performance, it is compared with existing methods such as DeepTxFinder (Zubow *et al.* (2020a)), CUTL (Mitchell *et al.* (2023a)), DSLoc (Liu, Zhang, Zhang, Zhang & Meng (2024b)), DeepMTL (Zhan *et al.* (2022)), and TL;DL (Mitchell, Baset, Patwari, Kasera & Bhaskara (2022b)) in Table 2.4.

Table 2.4 Comparison with state-of-the-art

Method	Key Features	Sensor Density	Average Error (in area of interest)	Measurement Device	Strengths	Weaknesses
DeepTxFinder Zubow, Bayhan, Gawłowicz & Dressler (2020b)	Deep learning for multiple transmitter localization; operates with unknown number of transmitters.	Sparse to moderate (1% - 2%)	10.1 m (in 14,400 m^2)	Crowdsourced USRPs	Scalable; does not need prior knowledge of transmitter power or count	High density regions require more computational resources.
CUTL Mitchell, Patwari, Bhaskara & Kasera (2023b)	Calibrated U-Net for transmitter localization; robust to OOD scenarios.	Moderate (2%)	40.1 m (in 4 km^2)	High-end SDRs: B210 and X310	Robust to heterogeneous sensors and environmental variability	Limited to datasets with high-quality calibration during training.
DSLoc Liu, Zhang, Zhang, Zhang & Meng (2024a)	Combines CNN and heatmap centroid-based localization for sparse WSNs.	Sparse (0.01% - 0.1%)	10.2 m (in 4 km^2)	High-end SDRs: B210 and X310	High-resolution grids; robust in extremely sparse networks	Challenges in real-time processing due to complex feature extraction.
DeepMTL Zhan *et al.* (2022)	YOLO-based transmitter localization with improved generalization over DeepTxFinder.	High (≥ 2%)	17 m (in 1 km^2)	Low-cost spectrum sensors	Strong generalization; handles complex environments well	Requires high density sensors for effectiveness; limited scalability.
TL;DL Mitchell, Baset, Patwari, Kasera & Bhaskara (2022a)	U-Net based localization with data augmentation for handling sparse sensor data.	Sparse (0.01%)	12.4 m (in 4,900 m^2)	Commodity wireless devices	Simple augmentation improves missing sensor scenarios	Accuracy decreases significantly in very large areas.
TxLocNet (proposed method)	Utilizes only border measurements for transmitter localization using ResNet; validated on real-world and simulated measurements.	Sparse (0.4%)	9.34 m (in 65,536 m^2)	Smartphone	Minimal data collection; robust to layout changes	Performance affected in highly obstructed scenarios without LoS; requires an approximate estimate of Tx power.

One of the primary differences between TxLocNet and other methods lies in sensor density and measurement strategy. Many methods, such as DeepMTL and DeepTxFinder, require moderate to high sensor densities to achieve reliable localization, often incorporating sophisticated deep learning architectures for transmitter localization. DeepMTL, for instance, uses a YOLO-based object detection approach to infer transmitter locations based on heatmaps. However, its reliance on high-density sensors limits its scalability to large, real-world deployments. DeepTxFinder, another deep-learning approach, partitions the coverage area into tiled regions to enhance computational efficiency while leveraging CNN models to predict the number and location of multiple transmitters. This technique is robust against environmental variations but computationally expensive.

TxLocNet, in contrast, operates in sparse sensor environments by focusing on border measurements. This approach allows for minimal data collection, making it suitable for scenarios where sensor deployment is constrained. Unlike DeepTxFinder and DeepMTL, TxLocNet does not rely on dense sensor grids or full-region heatmaps, making it a lightweight yet robust solution.

Another key differentiator is model robustness to environmental variability. CUTL, which employs a Calibrated U-Net, excels in handling out-of-distribution (OOD) data and heterogeneous sensor inputs. However, its reliance on high-quality calibration during training makes it less adaptable to environments where calibration data is unavailable. DSLoc, leveraging a heatmap centroid method based on High-Resolution Networks (HRNets), provides high-resolution localization accuracy, particularly in sparse Wireless Sensor Networks (WSNs), but struggles with real-time processing due to complex feature extraction requirements.

The strength of TxLocNet lies in its practical applicability as it leverages ResNet-based feature extraction to directly predict coordinates rather than relying on heatmaps or object detection approaches. This makes it resilient to layout changes and more adaptable to real-world deployments, especially where obstacles or NLoS conditions limit direct signal reception.

To the best of knowledge, TxLocNet is the first method that explores the localization of the transmitter by processing only the measurements of at the border of an area of interest. Even

though other SotA methods operate require measurements from locations scattered across the area of interest, the proposed method demonstrates comparable accuracy over them under otherwise similar conditions. By leveraging deep learning, the proposed model effectively maps spatial propagation characteristics of signals, enabling accurate localization with only minimal measurements.

A primary advantage of the proposed approach is its reduced data collection process. Relying solely on border measurements simplifies and accelerates the gathering of data, which is a considerable improvement in practical scenarios. Additionally, the deep learning model's ability to capture intricate signal propagation patterns contributes to high localization accuracy. This model has also shown promising adaptability across diverse environmental conditions and layout configurations, attributed to robust training practices. This makes it particularly valuable for use cases where measurement points are constrained to specific regions, such as monitoring wireless coverage along urban perimeters or within controlled environments where extensive sensor deployment is impractical.

It is important to note that none of the reviewed SotA methods, explicitly incorporate transmitter directionality as a modeled parameter, nor have they been evaluated under scenarios involving directional antennas. The same limitation applies to TxLocNet, which has been trained using the RadioMapSeer dataset, where signal propagation is simulated based on an omnidirectional transmitter. Consequently, if TxLocNet were to be applied in environments with directional transmitters, its localization performance would likely degrade. To enable effective localization in such scenarios, a new dataset would need to be developed, incorporating measurements from transmitters with varying radiation patterns and directional characteristics.

2.5.2 Ablation and Generalization Study

This section investigates the behavior of the TxLocNet model across different training and testing scenarios, offering insights that can guide future research.

2.5.2.1 Unknown Tx Power

In practical deployment scenarios, the exact Tx power might not be known. Since TxLocNet operates on input derived from received signal strength, its performance may be affected by inaccuracies in the assumed Tx power. To assess this sensitivity, an experiment is conducted using the measurement data from location a1 (from Table 2.3). The model was evaluated under varying assumed Tx power levels, and the resulting localization errors were recorded. As illustrated in Fig. 2.9, it was observed that the model is moderately sensitive to deviations in the assumed Tx power. When the assumed Tx power differed from the true value by less than ±3 dB, the Euclidean localization error remained within 40 m. These results indicate that although the model performs best with accurate Tx power information, it is capable of maintaining acceptable accuracy under small deviations.

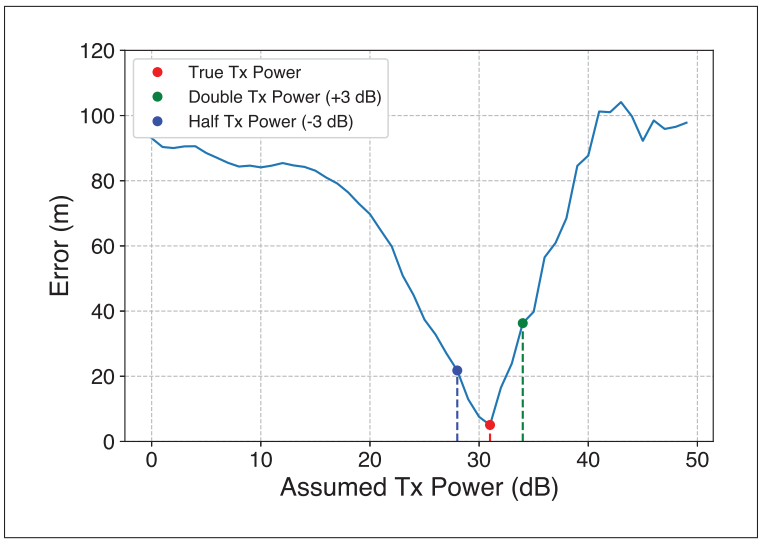

Figure 2.9 Euclidean Error vs. Assumed Tx power

2.5.2.2 Sparser Measurements

The default number of measurement points (256 points spaced at 1 m intervals) was selected based on the structure of the dataset, which provides path loss values corresponding to each pixel along the border. It is expected that the model performs optimally when all 256 measurement

points are available. To evaluate the sensitivity of TxLocNet to sparser measurements, an experiment was conducted using the real-world data from location a1 (referenced in Table 2.3).

In this experiment, only a subset of measurement points was retained, based on specified spacing intervals, and the remaining points were removed. Since TxLocNet requires an input of 256 values, the missing entries were reconstructed using linear interpolation. This approach allowed for a controlled evaluation of the model's performance under different sampling densities.

As shown in Table 2.5, when the spacing between measurements exceeds 10 m (i.e., fewer than 26 measurements along the 256 m path), the Euclidean localization error surpasses the 10% threshold (25.6 m). This indicates that, in this specific scenario, at least 26 evenly spaced measurements are needed to maintain acceptable localization accuracy.

Table 2.5 Effect of interpolation on TxLocNet performance

Distance between measurements (m)	1	2	5	10	15	20
No. of measurements	256	129	52	26	18	13
Error (m)	7.55	9.71	18.72	25.64	38.00	38.25

2.5.2.3 Dataset Augmentation

To enrich the dataset and potentially improve the performance of TxLocNet, the original RadioMapSeer dataset was augmented through rotational transformations. Each 256×256 radio map image was rotated by 90, 180, and 270 degrees, and the corresponding transmitter coordinates were adjusted accordingly. As a result, the dataset size increased from 56,000 to 224,000 samples. TxLocNet trained on the augmented dataset achieved an average localization error of 8.99 m, with a variance of 112.56 m^2. While this represents a modest improvement of approximately 0.44 m in average error (compared to the original 9.34 m), the training time increased significantly to over 22 hours and 15 minutes, using a server with specifications similar to those described in Section 2.3.2. Given the considerable increase in computational and

memory requirements, the marginal gain in accuracy does not justify the cost of augmentation in this case.

2.5.2.4 Measurements from Two Borders

To investigate whether incorporating an additional border could improve localization performance, an experiment was conducted in which the model was provided with both the right and top borders of each test sample. The final transmitter position was estimated by averaging the predictions from the two borders. While the overall Euclidean error remained 8.99 m, the axis-wise errors improved to 5.66 m along the x-axis and 5.76 m along the y-axis, indicating a modest enhancement in balance between the two dimensions. Despite this improvement, one of the primary motivations behind TxLocNet is to reduce the measurement burden in practical deployments. Collecting measurements along a single accessible path is significantly more feasible and scalable in outdoor environments compared to coordinating multiple borders, which would introduce additional logistical complexity, such as aligning measurement paths with different orientations. For this reason, TxLocNet is designed to achieve competitive accuracy using measurements from only a single border, making it more practical for real-world applications.

2.5.2.5 Separate Layouts in Training and Test

As described in Section 2.3.1, TxLocNet was initially trained using a random split of the full dataset, consisting of 70% for training, 15% for validation, and 15% for testing. This dataset included 56,000 samples generated from simulated radio maps covering 700 unique urban layouts, each with 80 transmitter positions. Under this random split, samples from the same layouts could appear in both training and test sets, which may allow the model to implicitly learn layout-specific features.

To investigate this possibility, a new dataset split was performed where layouts were separated across the training, validation, and test sets, maintaining the same 70/15/15 distribution. Using

this layout-separated split, the average test error increased from 9.34 m to 14.89 m. This result suggests that although the model benefits from prior exposure to layout characteristics in the original split, it is still capable of generalizing to previously unseen layouts, albeit with reduced accuracy.

It is acknowledged that the originally trained TxLocNet may have implicitly learned features related to the training layouts. Nonetheless, it achieves strong performance on real-world measurements, where the average localization error remains 7.23 m, indicating that the model retains practical utility even when applied to entirely new environments in measurement scenarios.

2.5.3 Practical Considerations and Limitations

TxLocNet's performance is influenced by assumptions in the RadioMapSeer dataset, such as omnidirectional transmitters and knowledge of transmit power within ±3 dB, though ablation studies show small deviations do not significantly affect accuracy. While trained at 5.9 GHz, the model achieved an average error of 7.23 m on real-world data at 2.6 GHz, demonstrating robustness to frequency shifts. The transmitter is assumed stationary and the receiver mobile, consistent with prior related localization research, and real-world measurements confirm no constraint on collection time. Moreover, experiments show acceptable accuracy with as few as 26 evenly spaced samples, allowing flexibility when dense sampling is infeasible. Although data-driven methods are inherently limited by their training simulations, TxLocNet avoids the need for detailed prior maps or building data required by rooftop propagation models, making it particularly useful where environmental knowledge is incomplete or inaccessible.

2.6 Conclusion

This paper introduces a machine learning-based method for solving transmitter localization problems in an area of interest using easily obtainable signal strength measurements at the border of that area. A central challenge in wireless networks is the ability to find the transmitter location

in complex outdoor environment with limited measurement and a cost-effective infrastructure. In outdoor scenarios, there are multiple buildings and obstructions which lead to attenuation, reflection, multipath, and occlusion. These prevent the use of traditional localization methods. In this work, a deep learning architecture based on ResNet is used to address the challenge of localization in a diverse set of complex environments, most importantly the user needs to acquire only one input vector with 256 signal strength measurements using a commercial smartphone. The model was trained using a publicly available dataset of simulated path loss using different set of environments and transmitter locations.

The model's performance on the test data set is better than the state of the art with average error of 9.34 m and standard deviation of 10.79 m. Furthermore, the model's performance is validated with measurements taken in urban environments. The results show the proposed model is able to accurately predict the transmitter location with an average error of 7.23 m with a standard deviation of 3.32 m.

Acknowledgments

The authors would like to thank Dr. Mathieu Gratuze for his support. We would like to acknowledge the contribution of the late Professor Charles Despins for the project initiation. This research was enabled in part by support provided by Calcul Québec (calculquebec.ca) and the Digital Research Alliance of Canada (alliancecan.ca).

CONCLUSION AND RECOMMENDATIONS

Summary of Key Findings

This research addressed the challenging problem of wireless transmitter localization in complex environments with limited access in terms of measurements, motivated by the growing need to efficiently manage networks and locate rogue transmitters in dense urban areas. Traditional techniques such as signal fingerprinting and triangulation struggle to perform in these scenarios, due to labor-intensive data collection and sensitivity to obstructions. To overcome these limitations, a novel approach using a deep ResNet was proposed for transmitter localization. The proposed model, TxLocNet, leverages only signal strength readings gathered along the perimeter of a 256×256 m^2 area as input. By employing the ResNet architecture's residual learning capabilities, the system learns complex propagation patterns and predicts the transmitter's coordinates within the area of interest without any prior knowledge of the environment's layout. This ResNet-based localization strategy reduces data requirements compared to conventional methods, since it eliminates the need for extensive in-area surveys.

Experiments and evaluations confirmed the effectiveness of the proposed approach. TxLocNet achieved high accuracy in pinpointing transmitter locations, outperforming or matching state-of-the-art methods. On a diverse simulated test set, the model attained a mean localization error of about 9.34 m (with a standard deviation of 10.79 m). Moreover, if only the measurements with Confidence index over 0.4 are considered, the mean localization error would decrease to 5.44 m with a 6.26 m standard deviation. This accuracy is on a par with than that of recent deep learning-based localization techniques, even those that utilize denser sensor deployments. For example, prior work like DeepTxFinder reported approximately 10 m error while relying on a sparse to moderate density (1% to 2%) of dedicated measurement devices spread throughout the area. In contrast, TxLocNet uses only boundary measurements (0.4% of the area's locations) to achieve sub-10 m error, while using only a smartphone as a device to gather measurement data.

The model's efficiency is also noteworthy – once trained, it produces location estimates almost instantaneously, making it suitable for real-time use. Empirical results on real-world data further demonstrated the approach's practicality: using live signal measurements at 2.7 GHz around a test area, the system localized the transmitter with an average error of about 7.23 m with a standard deviation of 3.32 m. This strong performance on both simulated and field data validates the ResNet-based approach as a reliable and accurate solution for transmitter localization.

Implications of the Research

This research explores a ResNet-based approach to wireless localization, addressing some challenges of traditional methods. Unlike fingerprinting, which requires extensive signal mapping, this approach collects data with a single border sweep. It also performs better than triangulation in non-line-of-sight conditions by accounting for signal obstructions and multipath effects. By relying on data-driven pattern recognition instead of analytical models, it provides localization using only a smartphone, without needing detailed knowledge of the environment or transmitter parameters.

The method has practical applications in network management, interference detection, and regulatory enforcement. It could help network operators optimize coverage and locate interference sources, while regulators might use it to identify unauthorized transmitters. Emergency responders could also benefit from its ability to estimate signal locations using perimeter-based measurements, even with mobile data collection via robots. The relatively low cost and minimal infrastructure requirements make it useful for both routine network tasks and emergency scenarios.

There are, however, some limitations. The approach may be less effective in highly obstructed environments where boundary signals provide limited information. It assumes a static environment, so moving transmitters or dynamic obstacles could impact accuracy. Physical

measurement collection may also be challenging in hazardous or remote areas. Additionally, adapting the model to different frequencies might require retraining. Despite these considerations, the research highlights how deep learning can be applied to localization and suggests areas for further improvement, particularly in dense urban or highly dynamic settings.

Future Research Directions

Building on the promising results of this work, several avenues for future research can be pursued to enhance TxLocNet's framework:

Scalability to Different Measurement Distances: One of the main challenges in real-world deployment is adapting the model to varying area sizes without retraining for each scenario. Future research could explore normalized input representations that scale measurement data according to the area's dimensions, allowing a single model to generalize across both small and large regions. A multi-resolution neural network approach (Wang *et al.* (2020)) could further enhance scalability by first estimating a broad transmitter region and then refining its position at a finer scale.

Adaptability to Different Frequencies: The current model was trained with data at 5.9 GHz and tested with measurements at 2.7 GHz, but real-world applications require localization across multiple frequencies, from sub-6 GHz cellular networks to millimeter wave (mmWave) and ultra high frequency (UHF) systems. Future work should focus on training with multi-frequency datasets and exploring transfer adaptation learning techniques (Zhang & Gao (2024)) to allow a single model to generalize across different signal propagation characteristics. Another promising direction is a hybrid frequency estimation approach, where the system first predicts the operating frequency band and then adjusts its localization strategy accordingly.

Robustness to Dynamic Environments: Many real-world localization scenarios involve time-varying conditions, where obstacles, people, or moving objects impact signal propagation.

To address this, incorporating signal strength measurements using recurrent neural networks (RNNs) could help the model adapt to evolving signal conditions over time. Reinforcement learning (RL) could also be explored to enable an adaptive localization strategy that improves accuracy based on feedback from previous predictions.

Academic Achievements

During this Master's degree, the following achievements have been obtained:

1. "A Residual Neural Network Approach to Transmitter Localization" by A. Ahmadi, A. Bhattacharya, F. Vaussenat, S. G. Cloutier, & R. Al Hadi, accepted by IEEE Transactions on Microwave Theory and Techniques (T-MTT) in October 2025.
2. "UNet-Based Deep Learning Pathloss Estimator with Boundary Condition Input" by A. Ahmadi, A. Bhattacharya, M. Gratuze, S. G. Cloutier, & R. Al Hadi, presented at IEEE Radio and Wireless Symposium (RWS) in January 2025.
3. "A Residual Neural Network Approach to Transmitter Localization" by A. Ahmadi, Z. Sepehri, M. Gratuze, M. Indja, A. Jemmali, V. Jevremovic, M. Lamontagne, S. G. Cloutier, I. Iordanova, C. Nerguizian, A. Motamedi & R. Al Hadi, presented at IEEE Radio and Wireless Symposium (RWS) in January 2024.

ANNEX A

WIRELESS NETWORK DEPLOYMENT SURVEY

Arash Ahmadi[1] , Zahra Sepehri[1] , Mathieu Gratuze[1] , Marouane Indja[2] , Ali Jemmali[3] , Vladan Jevremovic[3] , Marc-Antoine Lamontagne[3] , Sylvain G. Cloutier[1] , Ivanka Iordanova[2] , Chahé Nerguizian[4] , Ali Motamedi[2] , Richard Al Hadi[1]

[1] Département de Génie Électrique, École de Technologie Supérieure
[2] Département de Génie de la Construction, École de Technologie Supérieure
[3] Research and Development, iBwave Solutions
[4] Department of Electrical Engineering, Polytechnique Montréal

Conference paper published in proceedings of "IEEE Radio and Wireless Symposium (RWS)" in February 2024.

Abstract: This paper presents a study of an indoor wireless network based on modeling, electromagnetic (EM) simulation, and measurement. It combines Building Information Modeling (BIM) and EM to predict the channel characteristics of an area within the building. Data acquisition is performed to verify the BIM accuracy and to extract channel characteristics.

Keywords: wireless network, networks, 5G, urban areas, building construction, RF wave propagation, building information modeling, BIM, electromagnetic modeling, EM, channel characterization.

1. Introduction

The deployment of 5G networks in urban areas is accelerating to cover the need for higher data rates, ultra-low latency, and seamless connectivity for many devices. In an urban environment, it is challenging to achieve a direct line of sight between the base station and the users (Louro, Rui Fernandes, Rodrigues & Caldeirinha (2020)). This is caused by the complex and dense nature of buildings and structures (Al-Turjman, Lemayian, Alturjman & Mostarda (2019)). Urban areas present a unique environment where building construction materials, designs, and their layout significantly impact radio frequency (RF) wave propagation (Shafi *et al.* (2017); Matinmikko-Blue & Latva-aho (2017); Al-Turjman *et al.* (2019); Hosseini, Taleai & Zlatanova (2023)). These factors can lead to signal degradation, which adversely affects cellular coverage and performance. Ensuring reliable and robust network coverage in such environments requires a thorough understanding of the building characteristics and their influence on RF signals (Tariq, Despins, Affes & Nerguizian (2021)). To address these challenges, this paper focuses on the modeling, simulation, and measurement used in BIM in conjunction with EM simulation and channel characterization. In the following sections, we will cover the BIM and EM simulation flow, the data acquisition, and the findings and insights from this approach.

2. Physical Modeling

For an existing building, modeling starts with gathering data by exploring the architectural model and verifying its accuracy. This initial step is crucial as it lays the foundation for subsequent analysis and simulations. Ensuring the fidelity of the BIM model is essential to make informed decisions regarding wireless network deployment. This process involves dimensional verification, where physical measurements are taken to compare against the BIM model's dimensions. The starting model is shown in Figure-A A-1a. It presents some differences compared to the actual building mainly the absence of mechanical, electrical, and plumbing (MEP), structural beams, floor and ceiling data. The model was updated with elements present and crosschecked against the real structure shown in Figure-A A-1b by adding construction materials details as attributes

to enhance the representation accuracy. The model was then imported into iBwave Design Software.

The element used in the iBwave to model our setup was a generic signal source with WiFi 802.11.n technology operating at 2.4 GHz with the bandwidth of 20 MHz (channel 11) in the same location as the actual access point and the same height. The model also included an omnidirectional antenna operating at the same frequency range as the dipole antenna used in our measurements.

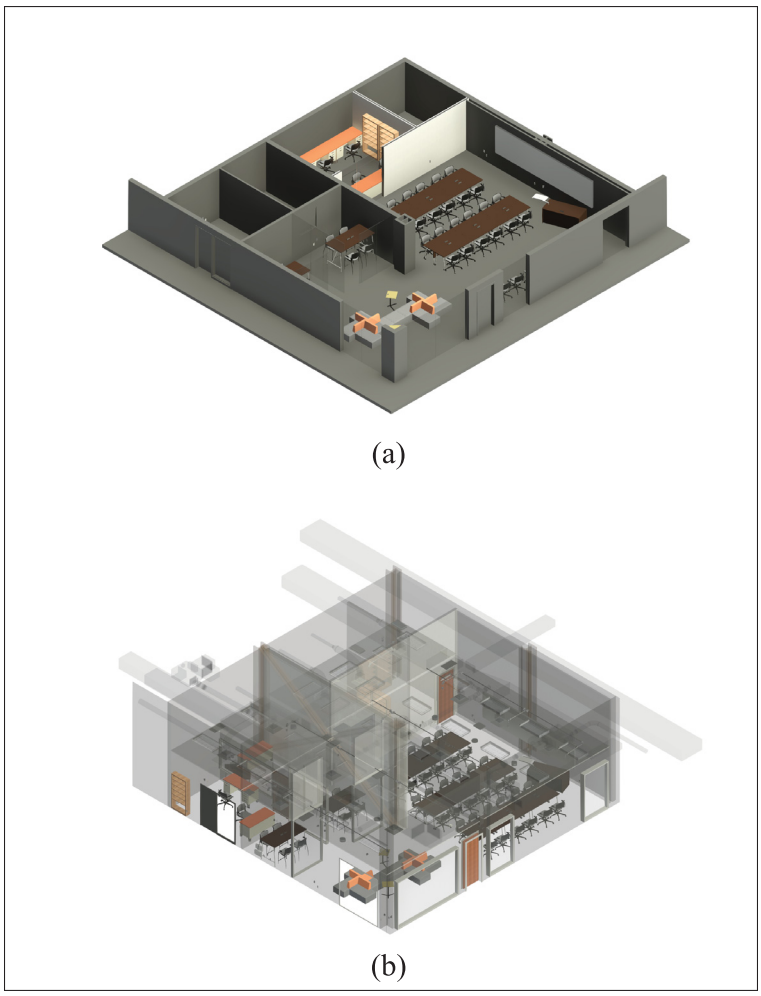

Figure-A A-1 Initially available model (a) and updated model after the verification survey (b)

3. RF Channel Modeling

Electromagnetic waves are subject to reflection, diffraction, and scattering from the propagation environment. Understanding the prevalent radio propagation characteristics is crucial in optimizing wireless communication systems (Rappaport (2002)). Consequently, channel characterization is necessary and can be achieved by modeling the channel with the complex impulse response in the time domain.

$$h(t,\tau) = \sum_{i=1}^{N(t)} a_i(t) e^{j\theta_i(t)} \delta(\tau - \tau_i(t)) \qquad \text{(A A-1)}$$

where $a_i(t)$, $\tau_i(t)$, and $\theta_i(t)$ are random variables expressing the amplitude, excess delay (arrival time), and phase sequences of different paths, respectively, while $N(t)$ is the number of multipath components at measurement instant t. $\delta(\cdot)$ represents the Dirac delta function, and i is the multipath component index (Rappaport (2002)).

$h(t,\tau)$ is used to calculate the Power Delay Profile (PDP). The PDP analysis serves to extract multipath parameters, including mean excess delay, RMS delay spread, and other relevant characteristics. These parameters play a critical role in not only comparing different multipath channels but also in laying the foundation for developing general design guidelines for wireless systems (Rappaport (2002)). Our research in this paper involved the extraction of these parameters from our wideband measurements, enabling a more comprehensive understanding of the channel's behavior and properties.

4. Measurements

Our survey focused on a small portion of the building of ÉTS campus, Montreal, QC, Canada. The selected area serves as a representative sample, capturing the complexities and variations that might exist throughout the entire building. This approach enables us to observe the changes in channel behavior and ensures the physical model remains up-to-date and is representative of the building's current state.

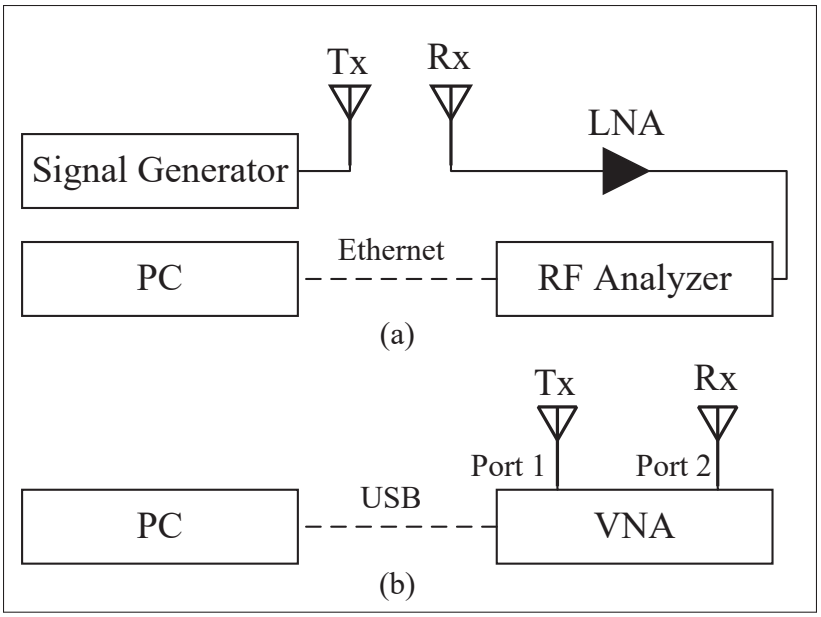

Figure-A A-2 Narrowband measurement setup (a) and wideband measurement setup (b)

The measurements to verify the EM simulation were conducted in two phases focusing on WiFi 802.11n signals at 2.4 GHz: Narrowband and wideband measurements.

4.1 Narrowband measurement setup and procedure

In order to establish a dependable data acquisition method, we used a Continuous Waves (CW) signal, transmitted using the E4438C ESG Vector Signal Generator (operating frequency of 250 kHz to 6 GHz, with the N9914A FieldFox RF Analyzer (operating frequency of 30 kHz to 6.5 GHz) serving as the receiver. A dual-band dipole antenna (RD-2458) was used at both the transmitter and receiver sides as demonstrated in Figure-A A-2a. The antennas were tested in an anechoic chamber at Polytechnique Montréal. Their gains and the propagation pattern were fairly consistent in the frequency range of 2.3-2.5 GHz. The transmitted signal operated at a fixed power level of 15dBm and the frequency of 2492 MHz. This frequency band was deliberately chosen outside of the WiFi standard spectrum to prevent interference from other channels. Additionally, a modulation scheme (BPSK) was applied to resemble WiFi signals. On the receiver side, the RF analyzer was connected to another dipole antenna (with the same

characteristics as the first antenna) through a Low Noise Amplifier (LNA). The LNA required a 12 V, 4 mA power supply. The channel power was determined using the RF analyzer at the same frequency with a 40 MHz span and a total of 401 data points. To control the RF analyzer and capture data, it was connected to a PC via an Ethernet cable. The signal generator remained stationary near the access point (AP), while the receiver was placed on a cart and moved to each measurement point, spaced one meter apart.

4.2 Wideband measurement setup and procedure

For wideband measurements, a Vector Network Analyzer (N5225A PNA Network Analyzer) with an operating frequency range from 10 MHz to 50 GHz was used to measure S-parameters. As depicted in Figure-A A-2b, the transmitter antenna was connected to port 1 of the VNA via a 1-meter cable, securely mounted on a tripod. Conversely, the receiver antenna was connected to port 2 of the VNA using a 20-meter cable and was also fixed to a tripod. The device was fully calibrated to account for the effect of cables and connectors. The VNA was interfaced with a PC and was controlled through a Python script. The antenna attached to port 1 remained fixed in place on its tripod, while the second antenna was relocated to each measurement point, the same locations used for narrowband measurements, also securely mounted on its tripod.

During data acquisition at each point, the magnitude and phase of the S21 parameter of that specific channel in the frequency domain were recorded. The PDP of the channel was obtained using the VNA's time domain feature. Subsequently, we performed post-processing analysis to extract key parameters such as RMS delay spread, mean excess delay, maximum excess delay, number of multipath components, relative multipath total power, arrival time of the first multipath component, and power of the first multipath component.

4.3 Results

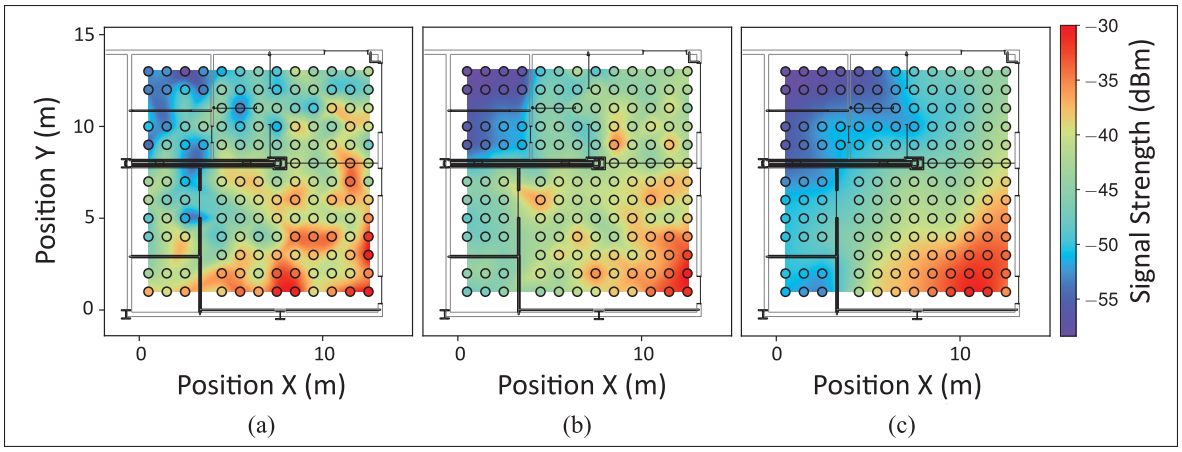

Figure-A A-3 Propagation maps in dBm (a) RSSI from narrowband measurements (b) relative multipath power from wideband measurements (c) RSSI from iBwave simulation

In Figure-A A-3, the Received Signal Strength Indicator (RSSI) from the normalized narrowband measurement is compared to the relative multipath total power from the wideband measurement and the RSSI from iBwave software simulation. The two measurement methods show very similar results according to Table-A A-1.

Table-A A-1 Difference between the simulation and measurements results

	Narrowband	**Wideband**
Mean Error	2.95 dBm	2.21 dBm
Absolute Mean Error	4.29 dBm	3.38 dBm
Standard Deviation	4.39 dBm	3.67 dBm

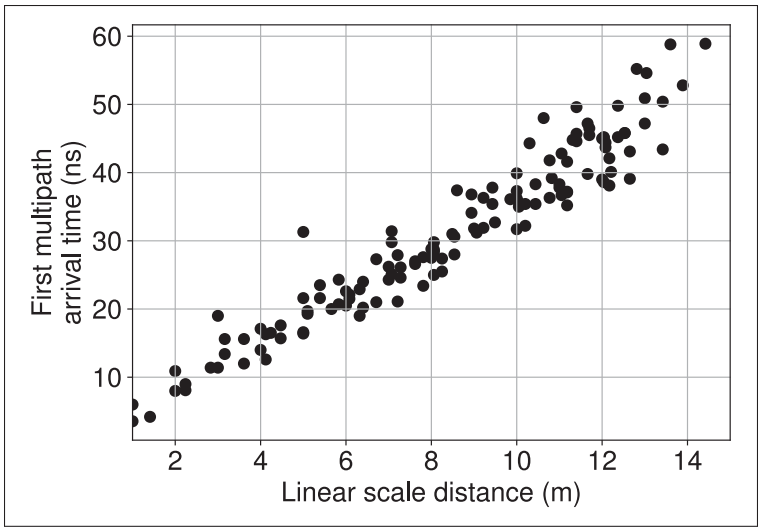

Figure-A A-4 Measured first multipath arrival time

It can also be observed that both measurements are consistent with iBwave simulation results. Other important parameters of the channel have been extracted from the wideband measurement. Figure-A A-4 shows the arrival time of the first multipath component versus the corresponding measurement location. The arrival times are consistent against values calculated using the speed of electromagnetic waves in the air. Figure-A A-5 demonstrates the relative total power of each measurement point. The slope of the line fitted to this data using linear regression is close to 1.78. This value is close to that of the free space which is 2 (Nerguizian, Despins, Affes & Djadel (2005)). Indoor environment may affect propagation resulting in a path loss exponent less than 2.

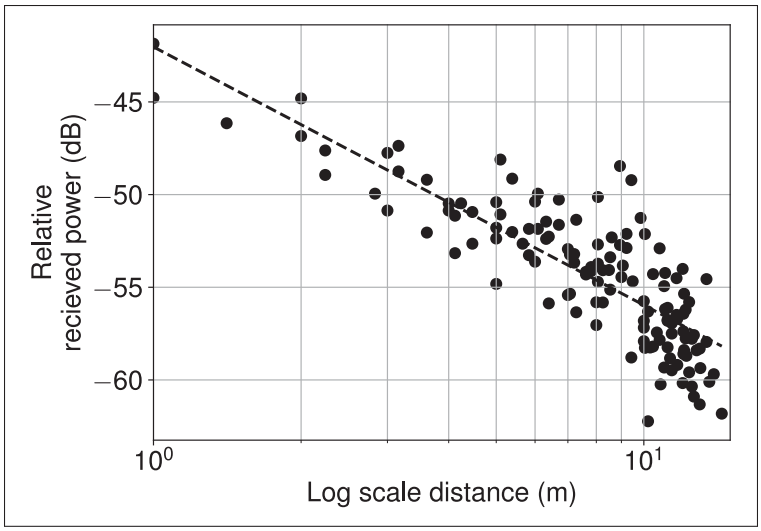

Figure-A A-5 Measured relative total power

The channel impulse response can be inspected in Figure-A A-6. Two points were considered for the measurement of impulse response: one with a direct Line Of Sight (LOS) and another one behind a "cross-brace" wall which is considered to have an Obstructed Line Of Sight (OLOS). Both points are at 13 meters distance from the transmitter antenna. The point with LOS observes the first peak at 50 ns and it can be associated with the direct path. The first peak arrives at the point with OLOS at 55 ns and the second peak arrives at 75 ns. The second peak can be attributed to a non-direct reflected path since it has a higher magnitude compared to the first one which is obstructed by the wall.

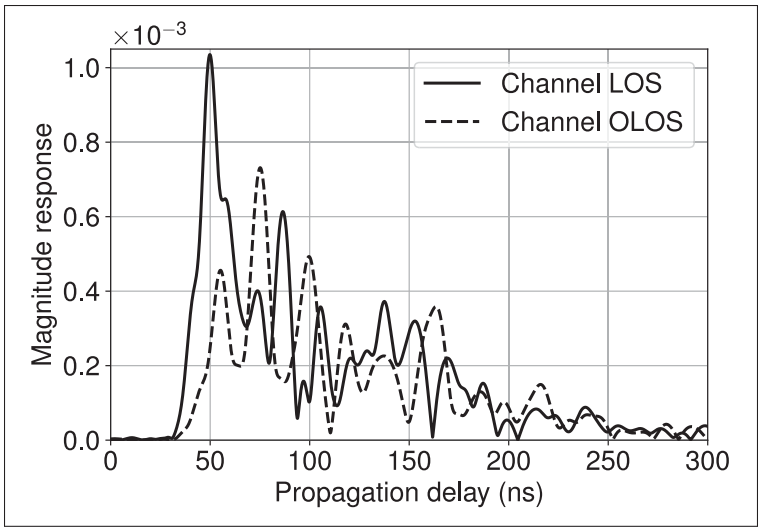

Figure-A A-6 Magnitude of the channel impulse response at the distance of 13 meters

5. Conclusion

Through this paper, we aim to demonstrate the impact of construction modeling in relation to wave propagation across a building for wireless network deployment. This study can be further extended to a wider range of channels and frequencies such as 5G and 6G network deployment in urban areas.

Acknowledgment

The authors would like to thank ÉTS Real Estate Projects Office, Philippe Leggett-Bachand, and Kevin Sicard from TELUS Montréal. The authors would like to acknowledge the contribution of the late Prof. Charles L. Despins for the project initiation.

ANNEX B

UNET-BASED DEEP LEARNING PATHLOSS ESTIMATOR WITH BOUNDARY CONDITION INPUT

Arash Ahmadi[1] , Abhiroop Bhattacharya[1] , Mathieu Gratuze[1] , Sylvain G. Cloutier[1] , Richard Al Hadi[1]

[1] Département de Génie Électrique, École de Technologie Supérieure,
1100 Notre-Dame Ouest, Montréal, Québec, Canada H3C 1K3

Conference paper published in proceedings of "IEEE Radio and Wireless Symposium (RWS)" in February 2025.

Abstract: This paper presents a UNet-based deep learning framework for pathloss estimation in wireless communication. Unlike traditional methods, this framework does not require knowledge of the source location. The model uses a boundary vector and a map as inputs to estimate the pathloss in a given area without the presence of a source. Our results show that the proposed model achieves accurate pathloss estimates at 5.9 GHz frequency band with a mean error of 0.35 dB compared to simulation values using a traditional dominant path model.

Keywords: Radio frequency, RF, propagation map, deep learning, UNet, convolutional neural network, CNN.

1. Introduction

Electromagnetic (EM) waves are subject to reflection, diffraction, and scattering from the environment, impacting the characteristics of radio wave propagation. Understanding these characteristics is crucial for optimizing wireless communication systems (Wahl, Wölfle, Wertz, Wildbolz & Landstorfer (2005)). *Pathloss* is a key metric that quantifies the attenuation in signal strength between a transmitter (T_X) and a receiver (R_X). It is defined as $P_L = (P_{R_X})_{dB} - (P_{T_X})_{dB}$, where P_{T_X} and P_{R_X} represent the transmitted power and received power at the T_X and R_X locations, respectively. The attenuation of signal power is caused by free-space propagation. In the absence of direct line of sight, reflection and diffraction from obstacles makes it difficult to estimate precisely P_L. This is an important analysis for the deployment of communication networks in urban areas where it is challenging to achieve a direct line of sight between T_X and R_X (Ahmadi *et al.* (2024)).

To address this challenge, several modeling techniques have been used in EM simulation and channel characterization. Firstly, *data driven interpolation* assumes that some measurements of P_L are given at some points. The methods in this category use some form of interpolation to estimate the P_L at the other locations. The common methods in this category are radial basis function interpolation, support vector regression, matrix completion (Chouvardas, Valentin, Draief & Leconte (2016)) and tensor completion (Schaufele, Cavalcante & Stanczak (2019)). The second category *Model based fitting* estimates P_L based on a prior assumptions on the physical system at non-measured locations. Thirdly, *model-based predictions* use only prior knowledge and physical systems without any measurements. The most widely used method is Ray tracing (Rautiainen, Wolfle & Hoppe (2002)), Dominant Path Model (DPM) (Wahl *et al.* (2005)) and empirical model.

Recently, neural networks have been explored to estimate P_L (Levie *et al.* (2021); Pyo, Sawada & Matsumura (2023)). However, the existing approaches require the exact source location and a fixed size layout map. As the complexity of urban layout maps become more

extensive, information such as wall thicknesses and partitions will get lost during the layout down-scaling to a predefined size, i.e. 256×256 pixels.

In an effort to solve these issues, we propose BoundaryUNet framework with the following advantages. Firstly, BoundaryUNet eliminates the need for precise T_X location information, making it highly adaptable to real-world scenarios where such data might be unavailable or difficult to obtain. Secondly, by leveraging boundary condition inputs, the model could extend P_L predictions to adjacent layouts, thereby providing a scalable solution for larger and more complex urban environments. This capability is crucial for efficient planning and optimization of wireless networks, especially in densely populated urban areas. Additionally, the use of the UNet architecture ensures high accuracy in P_L estimation while maintaining computational efficiency, making it suitable for real-time applications.

The paper is organized as follows: Section 2 introduces the proposed BoundaryUNet model, explaining its architecture and training methodology. Section 3 describes the dataset used for training and validation, Section 4 outlines the experimental setup and presents the results of our model's performance. Finally, in Section 5 a conclusion is given, it discusses the results drawn from this study and potential future work to further enhance P_L estimation methods.

2. Proposed Model

Our approach is based on the *RadioUNet* model proposed by Levie *et al.* (2021). We implement an approach that removes the need for precise transmitter coordinates. Furthermore, our approach can be extended in an iterative manner to get the propagation P_L of layouts with different sizes.

The model is based on the UNet architecture (Ronneberger, Fischer & Brox (2015)). UNets consist of convolution, pooling, up-sampling, and activation function layers, without fully connected layers. UNet is a deep learning architecture widely used for image segmentation tasks across various domains. It comprises an encoder-decoder structure with skip connections to preserve spatial information. The contracting path captures context, while the expanding path ensures precise localization. Its versatility and effectiveness make it popular for tasks such as

semantic segmentation in computer vision applications. In this model, we have two sequential UNets, the output of the first UNet is passed to the second UNet as shown in Figure-A B-1.

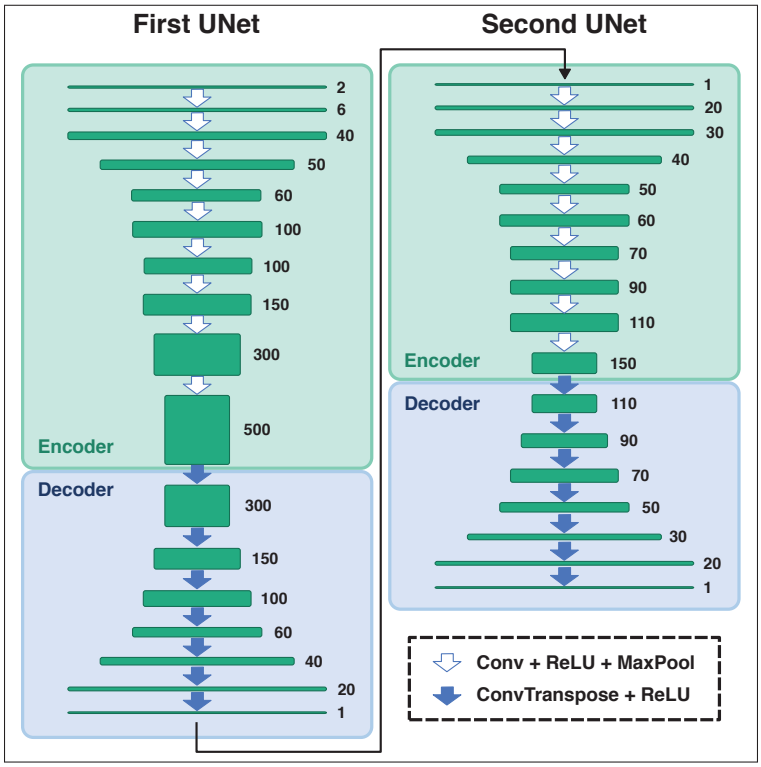

Figure-A B-1 BoundaryUNet layers and number of feature channels in each layer

In their original work, Levie *et al.* (2021) train their model using an image of the layout as the first input channel and the source location plotted in *(x,y)* coordinates as the second input channel. The target is the propagation map given the source and layout in the training data. The input channels and target are shown in Figure-A B-3 (a) and (b). The size of the model input channels and output is set to be 256 px × 256 px.

The intention of our work is to extend the propagation P_L from an original layout to an adjacent layout without knowledge of the transmitter location. In order to achieve this, we kept the layout input layer but replaced the second input layer to include P_L data from the border of the original layout, as shown in Figure-A B-3 (c) and (e). Figure-A B-3 (d) shows the target is the

propagation map given the layout and P_L data from the border in the training data. The size of the model input channels and output is set to be $128px \times 256px$. More detailed will be given in Section 3.

We then take this trained model and retrain it using an image which has the layout as the first channel and a blank image with the last two vectors of the propagation map to indicate the network profile of the source as shown if Figure-A B-2. This trained model is our final model which can be used with the last two vectors from a transmitter placed at any location. We call this model BoundaryUNet.

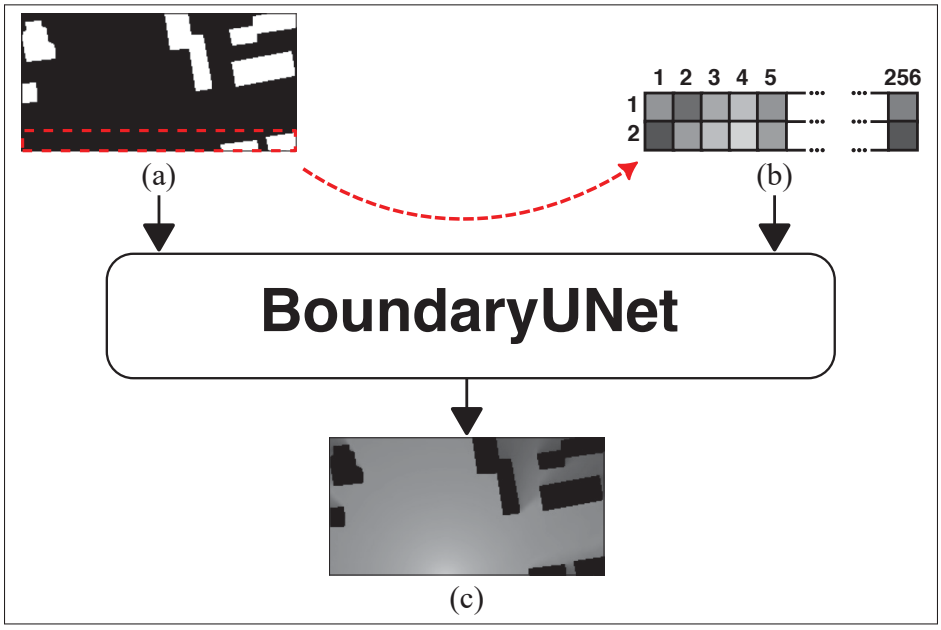

Figure-A B-2 BoundaryUNet (a) adjacent layout; (b) vectors containing P_L data from the border of the layout using simulation or measurement; (c) generated P_L data for the adjacent layout

We hypothesize that this approach can be repeated in an iterative manner to obtain the propagation map of layout maps with different sizes. The central assumption of our approach is that the last two vectors of the propagation map have sufficient information for the deep learning model to estimate the P_L accurately. The model is trained using the RadioMapSeer (Yapar *et al.* (2022)) dataset which is publicly available and was used by Levie *et al.* (2021).

3. Dataset

The RadioMapSeer (Yapar *et al.* (2022)) dataset includes 700 maps, each with 80 transmitter locations and corresponding simulated radio maps created using the DPM method. These maps are based on urban layouts from OpenStreetMap, featuring multiple cities worldwide. WinProp (Altair Engineering (2023)) software is used for the simulations, which are saved as densely sampled radio maps on a 2D grid. Buildings are stored as polygons and converted to a morphological 2D image where building interiors have a pixel value of 255 and exteriors have a pixel value of 0. Each layout is represented as a gray-scale image of 256 px $\times$ 256 px which corresponds to an area of 256×256 km^2. For this dataset, a signal bandwidth of 10 MHz in the 5.9 GHz band is considered. The choice of the 5.9 GHz frequency band is motivated by its relevance to device-to-device communications for safety in the context of intelligent transportation systems (ITS). This band is commonly used for vehicular communication systems, making it a pertinent choice for radio map estimation.

To convert P_L from the simulated radio maps to gray-scale pixel values ranging from 0 to 255, the following formula is used (Levie *et al.* (2021)):

$$GS = \frac{P_L - P_{L,trnc}}{M_1 - P_{L,trnc}} \times 255 \tag{A B-1}$$

where P_L is in dB. In RadioMapSeer dataset, M_1 represents the maximal P_L found in all radio maps, and $P_{L,trnc}$ is the P_L truncation threshold, which are considered as -47.84 dB and -147 dB, respectively. In this conversion, $GS = 0$ corresponds to values below the analytic noise floor, and $GS = 255$ denotes the maximum gain at the transmitter. Intermediate values between these extremes are represented as varying gray levels, effectively creating a gray-scale representation of P_L.

In order to train the model to extend propagation maps, a dataset is needed with the transmitter located outside of the map as shown in Figure-A B-3. This can be done by only considering a portion of RadioMapSeer dataset where the transmitter is located on the bottom half of the

map. The original dataset comprised of 700 layout maps, with 80 different antenna locations for each that resulted in a total of 56, 000 samples (or data points). In about 49.87% of the original dataset, the transmitter antenna is located on the bottom half of the map, but it is standard practice to make the dataset homogeneous (i.e. each layout having the same number of antenna locations). In order to do so, only 642 layout maps are considered with 33 transmitter locations thus reducing the total number of samples to 21, 186.

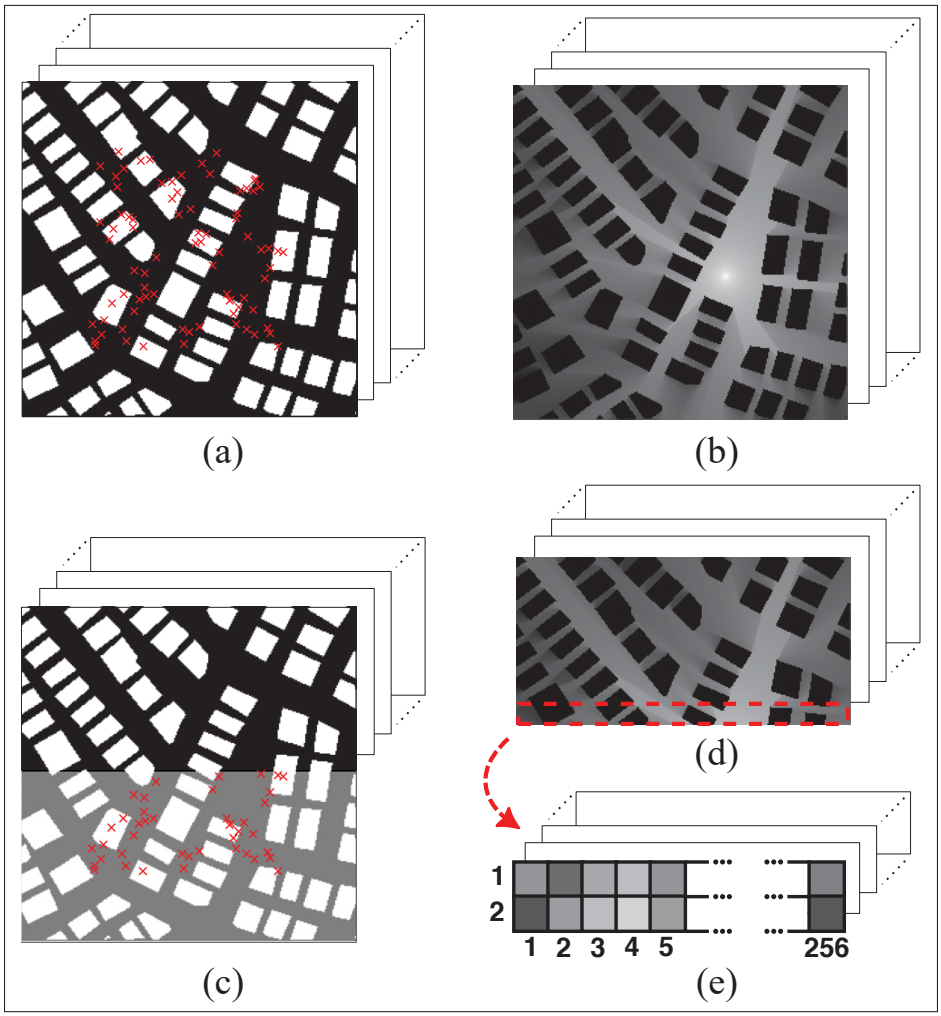

Figure-A B-3 Datasets: (a) maps from RadioMapSeer; (b) radio maps from RadioMapSeer; (c) top half of the maps with the Tx located outside (first input channel for BoundaryUNet); (d) corresponding radio maps (desired output for BoundaryUNet); (e) boundary vectors from radio maps (second input channel for BoundaryUNet)

4. Experiment

We have split the dataset so that 70% are assigned to training set, 15% to validation set and 15% to the testing set. The model is trained using supervised learning and MSE loss between the estimated propagation map and the simulated maps. We used the Adam optimizer with learning rate of 10^{-4}. Table-A B-1 shows the accuracy of BoundaryUNet on the test set after 50 epochs of training. It should be noted that the output of the model and its accuracy are both discrete and dimensionless. This is due to the encoding on a gray-scale of the P_L, for both WinProp and BoundaryUNet, the encoding is given by Equation A B-1. A repository containing the BoundaryUNet dataset, BoundaryUNet model, training and test scripts are uploaded to InteQX (2024).

Table-A B-1 BoundaryUNet accuracy on the test set

	First U	**Second U**
Mean Squared Error	2.95 dBm	2.21 dBm
Normalised Mean Squared Error	4.29 dBm	3.38 dBm

In order to test our trained model against simulation results, we fed the same layout to WinProp and BoundaryUNet. The results in Figure-A B-4a demonstrate that BoundaryUNet is capable of estimating nearly identical propagation P_L data compared to WinProp. The generated images are very similar in terms of direction of rays and shadows and there is only a slight blurring that occurs in light-shadow boundaries as shown in Figure-A B-4b presenting the relative error between the Winprop simulation of the output of the BoundaryUnet, hightlight the fact that the maximum relative error between the Winprop simulation and the output of BoundaryUNet is maximum 5 dB over a range of over 60 dB while being on average about 0.48 dB.

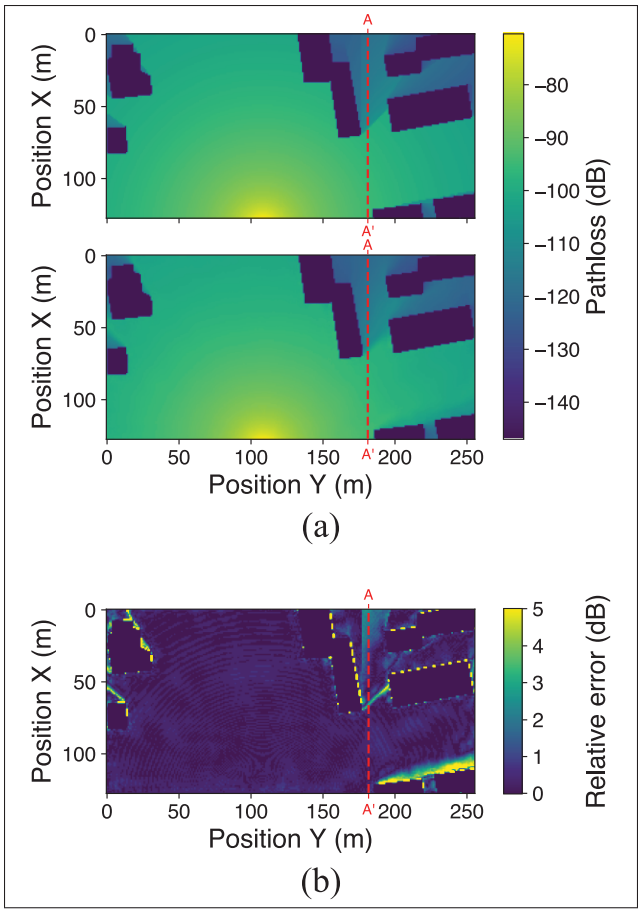

Figure-A B-4 Side by side propagation P_L: (a) WinProp simulation (top) vs. BoundaryUNet output (bottom); (b) relative error between simulation and model output

Overall, the precision of BoundaryUNet is proved by the slight difference between the results shown in Table-A B-2. Also to give a better picture of how the output of BoundaryUNet is close to the simulation results from Winprop, the propagation along the line A-A$'$ is shown in Figure-A B-5. This line allows the observation of the behavior of the P_L in Line of Sight (LoS) and Obstructed Line of Sight (OLoS) situations.

Table-A B-2 Difference between WinProp simulation and BoundaryUNet results

	Value (dB)
Mean Error	0.3509
Absolute Mean Error	0.4782
Standard Deviation	2.2157

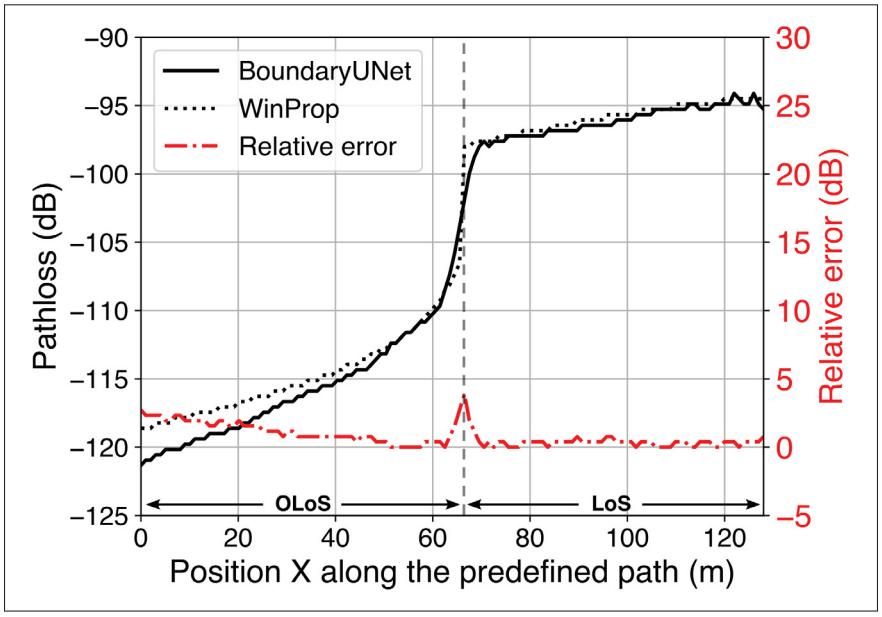

Figure-A B-5 Comparison of P_L between WinProp simulation and BoundaryUNet output along the Line A-A′

This figure also highlights the fact that the relative error between the Winprop simulation and the output of BoundaryUNet is relatively constant over the line A-A′, and thus the distance does not affect the observed error. However, the transition from LoS to OLoS condition does lead to a local increase of the relative error.

5. Conclusion

In this paper we designed a deep learning framework based on UNet that estimates propagation map for a layout, regardless of the transmitter antenna location. To the best of our knowledge, this is this first work which explores the application of machine learning for estimating path loss without any knowledge of the transmitter location. Instead it requires the P_L data along one border of the layout and extends it to the whole layout. The proposed model is not restricted to a fixed size layout and can model large complex spaces using the boundary vector which is an inherent limitation of deep learning models. One practical use case for this framework is when we want to extend an already available propagation P_L map. Another scenario where BoundaryUNet can be useful is when transmitter antenna is located outside of the layout, and we want to acquire propagation P_L data across the layout. In this case, We only need to have the P_L data along one of the layout boundaries. For instance, in a real world scenario, this can be used for estimating the optimal transmitter placement inside large buildings with detailed plans.

To further enhance the capabilities of the BoundaryUNet framework, future research could explore several promising directions. Integrating real-time feedback from deployed wireless networks could enable the model to dynamically adjust its predictions based on actual performance data, leading to continuous improvement in P_L estimation. Additionally, a comprehensive framework could be developed to generate the propagation P_L map for large and detailed layouts using BoundaryUNet, thereby facilitating its application in extensive urban environments. Another significant avenue for advancement is the integration of different material properties, such as metal, concrete, wood, and glass, into the model, similar to what has been done in (Pyo *et al.* (2023)). This would enable the generation of more accurate P_L data by accounting for the specific propagation characteristics of various building materials. These enhancements would collectively contribute to a more robust and versatile P_L estimation tool, suitable for a wide range of real-world applications.

Acknowledgment

We would like to thank P. Leggett-Bachand from Telus; M. Lamontagne, Dr. V. Jevremovic Dr. A. Jemmali from iBwave; Prof. I. Iordanova and Prof. A. Motamedi from ÉTS. We acknowledge the contribution of the late Prof. Charles Despins for the project initiation.

LIST OF REFERENCES

Ahmadi, A., Sepehri, Z., Gratuze, M., Indja, M., Jemmali, A., Jevremovic, V., Lamontagne, M.-A., Cloutier, S. G., Iordanova, I., Nerguizian, C., Motamedi, A. & Al Hadi, R. (2024, Jan). Wireless Network Deployment Survey. *2024 IEEE Radio and Wireless Symposium (RWS)*, pp. 143–146. doi: 10.1109/RWS56914.2024.10438583.

Ahmadi, A., Bhattacharya, A., Gratuze, M., Cloutier, S. G. & Hadi, R. A. (2025a). UNet-Based Deep Learning Pathloss Estimator with Boundary Condition Input. *IEEE Radio and Wireless Symp.*, pp. 9–12.

Ahmadi, A., Bhattacharya, A., Vaussenat, F., Cloutier, S. G. & Al Hadi, R. (2025b, Feb). A Residual Neural Network Approach to Transmitter Localization (Version v1). Retrieved from: https://codeocean.com/capsule/8795732/tree/v1.

Al-Turjman, F., Lemayian, J. P., Alturjman, S. & Mostarda, L. (2019). Enhanced Deployment Strategy for the 5G Drone-BS Using Artificial Intelligence. *IEEE Access*, 7, 75999–76008. doi: 10.1109/ACCESS.2019.2921729.

Alagha, A., Mizouni, R., Singh, S., Bentahar, J. & Otrok, H. (2025). Adaptive target localization under uncertainty using Multi-Agent Deep Reinforcement Learning with knowledge transfer. *Internet of Things*, 29, 101447. doi: 10.1016/j.iot.2024.101447.

Altair Engineering. [Publication Title: Default]. (2023). Altair Feko, Radio Coverage Planning, Wireless Networks, Including 5G, 2023. Retrieved on 2024-07-17 from: https://web.altair.com/winprop-telecom.

Alzubaidi, L., Zhang, J., Humaidi, A. J., Al-Dujaili, A., Duan, Y., Al-Shamma, O., Santamaría, J., Fadhel, M. A., Al-Amidie, M. & Farhan, L. (2021). Review of deep learning: concepts, CNN architectures, challenges, applications, future directions. *Journal of Big Data*, 8(1), 53. doi: 10.1186/s40537-021-00444-8.

Andersson, M., Lidström, A. & Lindmark, G. (2023, Apr). Indoor 5G Positioning using Multipath Measurements. *2023 IEEE/ION Position, Location and Navigation Symposium (PLANS)*, pp. 1092–1098. doi: 10.1109/PLANS53410.2023.10140035.

Bahl, P. & Padmanabhan, V. (2000). RADAR: an in-building RF-based user location and tracking system. *Proceedings IEEE INFOCOM 2000. Conference on Computer Communications. Nineteenth Annual Joint Conference of the IEEE Computer and Communications Societies (Cat. No.00CH37064)*, 2, 775–784. doi: 10.1109/INFCOM.2000.832252.

Cao, Y., Lv, T., Lin, Z., Huang, P. & Lin, F. (2020). Complex ResNet Aided DoA Estimation for Near-Field MIMO Systems. *IEEE Transactions on Vehicular Technology*, 69(10), 11139–11151. doi: 10.1109/tvt.2020.3007894. Publisher: Institute of Electrical and Electronics Engineers (IEEE).

Chang, L., Xiong, J., Wang, Y., Chen, X., Hu, J. & Fang, D. (2017, Jun). iUpdater: Low Cost RSS Fingerprints Updating for Device-Free Localization. *2017 IEEE 37th International Conference on Distributed Computing Systems (ICDCS)*, pp. 900–910. doi: 10.1109/ICDCS.2017.216.

Chen, H.-C., Lin, T.-H., Kung, H. T., Lin, C.-K. & Gwon, Y. (2012, Oct). Determining RF angle of arrival using COTS antenna arrays: A field evaluation. *MILCOM 2012 - 2012 IEEE Military Communications Conference*, pp. 1–6. doi: 10.1109/MILCOM.2012.6415851.

Chen, J., Zhao, R., Yang, C. & Dai, Y. (2023, Jun). Wireless Signal Recognition Based on ResNet-Transformer. *2023 11th International Conference on Intelligent Computing and Wireless Optical Communications (ICWOC)*, pp. 1–6. doi: 10.1109/icwoc57905.2023.10200835.

Cho, E. K. & Simsek, E. (2024). Enhancing the Resolution of Local Near-Field Probing Measurements With Machine Learning. *IEEE Transactions on Microwave Theory and Techniques*, 72(3), 1515–1519. doi: 10.1109/TMTT.2023.3312036.

Chouvardas, S., Valentin, S., Draief, M. & Leconte, M. (2016, Mar). A method to reconstruct coverage loss maps based on matrix completion and adaptive sampling. *2016 IEEE International Conference on Acoustics, Speech and Signal Processing (ICASSP)*, pp. 6390–6394. doi: 10.1109/ICASSP.2016.7472907.

Chuang, S.-F., Wu, W.-R. & Liu, Y.-T. (2015). High-Resolution AoA Estimation for Hybrid Antenna Arrays. *IEEE Trans. Antennas Propagation*, 63(7), 2955-2968. doi: 10.1109/TAP.2015.2426795.

Dou, F., Lu, J., Zhu, T. & Bi, J. (2024). On-Device Indoor Positioning: A Federated Reinforcement Learning Approach With Heterogeneous Devices. *IEEE Internet of Things Journal*, 11(3), 3909–3926. doi: 10.1109/JIOT.2023.3299262.

Elsanhoury, M., Mäkelä, P., Koljonen, J., Välisuo, P., Shamsuzzoha, A., Mantere, T., Elmusrati, M. & Kuusniemi, H. (2022). Precision Positioning for Smart Logistics Using Ultra-Wideband Technology-Based Indoor Navigation: A Review. *IEEE Access*, 10, 44413-44445. doi: 10.1109/ACCESS.2022.3169267.

ETSI. (2020, Feb). LTE; E-UTRA; UE radio transmission and reception (3GPP TS 36.101 ver. 15.9.0 Release 15). Retrieved from: Eur.Telecommun.StandardsInst.

ETSI. (2020, Dec). LTE; E-UTRA; Requirements for Support of Radio Resource Management (3GPP TS 36.133 version 16.7.0 Release 16). Retrieved from: Eur.Telecommun. StandardsInst.

Fan, Y. & Sun, H. (2024). Environmental causality calibration: Advancing WLAN RF fingerprinting for precise indoor localization. *PLOS ONE*, 19(2), e0297108. doi: 10.1371/journal.pone.0297108.

Guo, Z., Sun, Y., Jian, M. & Zhang, X. (2018). Deep Residual Network with Sparse Feedback for Image Restoration. *Applied Sciences*, 8(12), 2417. doi: 10.3390/app8122417.

He, K., Zhang, X., Ren, S. & Sun, J. (2016, Jun). Deep Residual Learning for Image Recognition. *IEEE Conf. on Comput. Vis. and Pattern Recognit. (CVPR)*, pp. 770–778. doi: 10.1109/CVPR.2016.90.

He, S. & Dong, X. (2017). High-Accuracy Localization Platform Using Asynchronous Time Difference of Arrival Technology. *IEEE Trans. on Instrumentation and Measurement*, 66(7), 1728-1742. doi: 10.1109/TIM.2017.2666278.

Hoppe, R., Wolfle, G. & Jakobus, U. (2017, Mar). Wave propagation and radio network planning software WinProp added to the electromagnetic solver package FEKO. *Int. Appl. Comput. Electromagn. Soc. Symp. (ACES)*, pp. 1–2. doi: 10.23919/ROPACES.2017.7916282.

Horansky, R. D., Coder, J. B. & Ladbury, J. M. (2019). *LTE handset emissions:*.

Hosseini, H., Taleai, M. & Zlatanova, S. (2023). NSGA-II based optimal Wi-Fi access point placement for indoor positioning: A BIM-based RSS prediction. *Automation in Construction*, 152, 104897. doi: 10.1016/j.autcon.2023.104897.

InteQX. (2024). BoundaryUNet. Retrieved from: https://github.com/inteqx/BoundaryUnet.

Jagannath, A. & Jagannath, J. (2020, Dec). Jam-Guard: Low-Cost, Hand-held Device for First Responders to Detect and Localize Jammers. *2020 14th International Conference on Signal Processing and Communication Systems (ICSPCS)*, pp. 1–7. doi: 10.1109/ICSPCS50536.2020.9310004.

Jang, J.-W. & Hong, S.-N. (2018, Jul). Indoor Localization with WiFi Fingerprinting Using Convolutional Neural Network. *2018 Tenth International Conference on Ubiquitous and Future Networks (ICUFN)*, pp. 753–758. doi: 10.1109/ICUFN.2018.8436598.

Junoh, S. A. & Pyun, J.-Y. (2024). Augmentation of Fingerprints for Indoor BLE Localization Using Conditional GANs. *IEEE Access*, 12, 30176–30190. doi: 10.1109/ACCESS.2024.3368449.

Khoo, H. W., Ng, Y. H. & Tan, C. K. (2022). Enhanced Radio Map Interpolation Methods Based on Dimensionality Reduction and Clustering. *Electronics*, 11(16), 2581. doi: 10.3390/electronics11162581.

Kingma, D. P. & Ba, J. (2015). Adam: A Method for Stochastic Optimization. *Int. Conf. on Learning Representations*.

Kuruvatti, N. P., Habibi, M. A., Partani, S., Han, B., Fellan, A. & Schotten, H. D. (2022). Empowering 6G Communication Systems With Digital Twin Technology: A Comprehensive Survey. *IEEE Access*, 10, 112158–112186. doi: 10.1109/ACCESS.2022.3215493.

Lecun, Y., Bottou, L., Bengio, Y. & Haffner, P. (1998). Gradient-based learning applied to document recognition. *Proc. of the IEEE*, 86(11), 2278–2324. doi: 10.1109/5.726791.

Lee, H., Kang, T., Jeong, S. & Seo, J. (2022, Jun). Evaluation of RF Fingerprinting-Aided RSS-Based Target Localization for Emergency Response. *2022 IEEE 95th Vehicular Technology Conference: (VTC2022-Spring)*, pp. 1–7. doi: 10.1109/VTC2022-Spring54318.2022.9860436.

Levie, R., Yapar, C., Kutyniok, G. & Caire, G. (2021). RadioUNet: Fast Radio Map Estimation With Convolutional Neural Networks. *IEEE Transactions on Wireless Communications*, 20(6), 4001–4015. doi: 10.1109/TWC.2021.3054977.

Li, Y., Hu, X., Zhuang, Y., Gao, Z., Zhang, P. & El-Sheimy, N. (2020). Deep Reinforcement Learning (DRL): Another Perspective for Unsupervised Wireless Localization. *IEEE Internet of Things Journal*, 7(7), 6279–6287. doi: 10.1109/JIOT.2019.2957778.

Liu, R., Zhang, Q., Zhang, Y., Zhang, R. & Meng, T. (2024a). Deep Learning-Based Transmitter Localization in Sparse Wireless Sensor Networks. *Sensors*, 24(16). doi: 10.3390/s24165335.

Liu, R., Zhang, Q., Zhang, Y., Zhang, R. & Meng, T. (2024b). Deep Learning-Based Transmitter Localization in Sparse Wireless Sensor Networks. *Sensors*, 24(16), 5335. doi: 10.3390/s24165335.

Louro, J. S., Rui Fernandes, T., Rodrigues, H. & Caldeirinha, R. F. S. (2020, Jul). 3D Indoor Radio Coverage for 5G Planning: a Framework of Combining BIM with Ray-tracing. *2020 12th International Symposium on Communication Systems, Networks and Digital Signal Processing (CSNDSP)*, pp. 1–5. doi: 10.1109/CSNDSP49049.2020.9249503.

Lu, M., Xiao, X., Pang, Y., Liu, G. & Lu, H. (2022). Detection and Localization of Breast Cancer Using UWB Microwave Technology and CNN-LSTM Framework. *IEEE Transactions on Microwave Theory and Techniques*, 70(11), 5085–5094. doi: 10.1109/TMTT.2022.3209679.

Luo, R., Wang, L., He, Z., Xiao, F., Xiao, L.-Y. & Liu, Q. H. (2024). A Wideband and Flexible Testing System Based on a Quasi-Coaxial Structure and Machine Learning. *IEEE Transactions on Microwave Theory and Techniques*, 72(3), 1766–1774. doi: 10.1109/TMTT.2023.3311957.

Matinmikko-Blue, M. & Latva-aho, M. (2017, Dec). Micro operators accelerating 5G deployment. *2017 IEEE International Conference on Industrial and Information Systems (ICIIS)*, pp. 1–5. doi: 10.1109/ICIINFS.2017.8300396.

Mitchell, F., Baset, A., Patwari, N., Kasera, S. K. & Bhaskara, A. (2022a). Deep Learning-based Localization in Limited Data Regimes. *Proc. of the 2022 ACM Workshop on Wireless Secur. and Mach. Learn.*, (WiseML '22), 15–20. doi: 10.1145/3522783.3529529.

Mitchell, F., Baset, A., Patwari, N., Kasera, S. K. & Bhaskara, A. (2022b). Deep Learning-based Localization in Limited Data Regimes. *ACM Workshop on Wireless Secur. and Machine Learning*, pp. 15–20. doi: 10.1145/3522783.3529529.

Mitchell, F., Patwari, N., Bhaskara, A. & Kasera, S. K. (2023a). Learning-based Techniques for Transmitter Localization: A Case Study on Model Robustness. *IEEE Int. Conf. on Sensing, Communication, and Networking*, pp. 133-141. doi: 10.1109/SECON58729.2023.10287483.

Mitchell, F., Patwari, N., Bhaskara, A. & Kasera, S. K. (2023b). Learning-based Techniques for Transmitter Localization: A Case Study on Model Robustness. *Annu. IEEE Int. Conf. on Sens., Commun., and Netw. (SECON)*, pp. 133–141. doi: 10.1109/SECON58729.2023.10287483.

Nerguizian, C., Despins, C., Affes, S. & Djadel, M. (2005). Radio-channel characterization of an underground mine at 2.4 GHz. *IEEE Transactions on Wireless Communications*, 4(5), 2441–2453. doi: 10.1109/TWC.2005.853899.

Ning, Z., Vandersteegen, M., Van Beeck, K., Goedemé, T. & Vandewalle, P. (2024). Power Consumption Benchmark for Embedded AI Inference. *Int. Conf. on Applied Computing*.

Nurminen, H., Dashti, M. & Piché, R. (2017). A survey on wireless transmitter localization using signal strength measurements. *Wireless Commun. and Mobile Comput.*, 2017(1), 1–12. Publisher: Wiley Online Library.

Osa, V., Matamales, J., Monserrat, J. F. & López, J. (2013). Localization in Wireless Networks: The Potential of Triangulation Techniques. *Wireless Pers. Commun.*, 68(4), 1525–1538. doi: 10.1007/s11277-012-0537-2.

Pyo, C., Sawada, H. & Matsumura, T. (2023). A Deep Learning-Based Indoor Radio Estimation Method Driven by 2.4 GHz Ray-Tracing Data. *IEEE Access*, 11, 138215–138228. doi: 10.1109/ACCESS.2023.3340204.

Rappaport, T. (2001). *Wireless Communications: Principles and Practice* (ed. 2nd). Prentice Hall PTR.

Rappaport, T. (2002). *Wireless Communications: Principles and Practice* (ed. 2nd). Prentice Hall PTR.

Rautiainen, T., Wolfle, G. & Hoppe, R. (2002). Verifying path loss and delay spread predictions of a 3D ray tracing propagation model in urban environment. *Proceedings IEEE 56th Vehicular Technology Conference*, 4, 2470–2474. doi: 10.1109/VETECF.2002.1040665.

Rojhani, N., Passafiume, M., Sadeghibakhi, M., Collodi, G. & Cidronali, A. (2023). Model-Based Data Augmentation Applied to Deep Learning Networks for Classification of Micro-Doppler Signatures Using FMCW Radar. *IEEE Trans. Microwave Theory and Techniques*, 71(5), 2222-2236. doi: 10.1109/TMTT.2023.3231371.

Ronneberger, O., Fischer, P. & Brox, T. (2015). U-Net: Convolutional Networks for Biomedical Image Segmentation. *Medical Image Computing and Computer-Assisted Intervention – MICCAI 2015*, pp. 234–241.

Sandler, M., Howard, A., Zhu, M., Zhmoginov, A. & Chen, L.-C. (2018, Jun). MobileNetV2: Inverted Residuals and Linear Bottlenecks. *IEEE/CVF Conf. on Comput. Vis. and Pattern Recognit.*, pp. 4510–4520. doi: 10.1109/CVPR.2018.00474.

Schaufele, D., Cavalcante, R. L. G. & Stanczak, S. (2019, Jul). Tensor Completion for Radio Map Reconstruction using Low Rank and Smoothness. *2019 IEEE 20th International Workshop on Signal Processing Advances in Wireless Communications (SPAWC)*, pp. 1–5. doi: 10.1109/SPAWC.2019.8815495.

Shafi, M., Molisch, A. F., Smith, P. J., Haustein, T., Zhu, P., De Silva, P., Tufvesson, F., Benjebbour, A. & Wunder, G. (2017). 5G: A Tutorial Overview of Standards, Trials, Challenges, Deployment, and Practice. *IEEE Journal on Selected Areas in Communications*, 35(6), 1201–1221. doi: 10.1109/JSAC.2017.2692307.

Shafiq, M. & Gu, Z. (2022). Deep Residual Learning for Image Recognition: A Survey. *Applied Sciences*, 12(18), 8972. doi: 10.3390/app12188972.

Sun, Y., Yang, S., Wang, G. & Chen, H. (2021). Robust RSS-Based Source Localization With Unknown Model Parameters in Mixed LOS/NLOS Environments. *IEEE Trans. Vehicular Technology*, 70(4), 3926-3931. doi: 10.1109/TVT.2021.3064444.

Tariq, S. A. M., Despins, C. L., Affes, S. & Nerguizian, C. (2021). Characterization of a 60 GHz scattered wireless channel with different antenna polarizations for underground multimedia applications. *IET Microwaves, Antennas & Propagation*, 15(9), 1063–1075. doi: 10.1049/mia2.12116.

Wahl, R. & Wolfle, G. (2006, Nov). Combined urban and indoor network planning using the dominant path propagation model. *Eur. Conf. on Antennas and Propag.*, pp. 1–6. doi: 10.1109/EUCAP.2006.4584790.

Wahl, R., Wölfle, G., Wertz, P., Wildbolz, P. & Landstorfer, F. (2005). Dominant Path Prediction Model for Urban Scenarios. *IST MWC*, pp. 1–5.

Wang, C., Zheng, X., Chen, Y. & Yang, J. (2017). Locating Rogue Access Point Using Fine-Grained Channel Information. *IEEE Trans. on Mobile Computing*, 16(9), 2560-2573. doi: 10.1109/TMC.2016.2629473.

Wang, F., Eljarrat, A., Müller, J., Henninen, T. R., Erni, R. & Koch, C. T. (2020). Multi-resolution convolutional neural networks for inverse problems. *Scientific Reports*, 10(1), 5730. doi: 10.1038/s41598-020-62484-z.

Xie, S., Girshick, R., Dollár, P., Tu, Z. & He, K. (2017). Aggregated Residual Transformations for Deep Neural Networks. *IEEE Conf. on Comput. Vis. and Pattern Recognit. (CVPR)*, pp. 5987–5995. doi: 10.1109/CVPR.2017.634.

Yapar, C., Levie, R., Kutyniok, G. & Caire, G. (2022). Dataset of Pathloss and ToA Radio Maps with Localization Application. IEEE DataPort. Retrieved on 2025-02-24 from: https://ieee-dataport.org/documents/radiomapseer.

Yaro, A. S., Maly, F. & Prazak, P. (2023). A Survey of the Performance-Limiting Factors of a 2-Dimensional RSS Fingerprinting-Based Indoor Wireless Localization System. *Sensors*, 23(5), 2545. doi: 10.3390/s23052545.

Ye, Y. & Wang, B. (2018). RMapCS: Radio Map Construction From Crowdsourced Samples for Indoor Localization. *IEEE Access*, 6, 24224–24238. doi: 10.1109/ACCESS.2018.2830415.

Yen, H.-C., Ou Yang, L.-Y. & Tsai, Z.-M. (2022). 3-D Indoor Localization and Identification Through RSSI-Based Angle of Arrival Estimation With Real Wi-Fi Signals. *IEEE Trans. Microwave Theory and Techniques*, 70(10), 4511-4527. doi: 10.1109/TMTT.2022.3194563.

Zagoruyko, S. & Komodakis, N. (2016, Sep). Wide Residual Networks. *Proceedings of the British Machine Vision Conference (BMVC)*, pp. 1–12. doi: 10.5244/C.30.87.

Zhan, C., Ghaderibaneh, M., Sahu, P. & Gupta, H. (2022). DeepMTL Pro: Deep Learning Based Multiple Transmitter Localization and Power Estimation. *Pervasive and Mobile Comput.*, 82, 101582. doi: https://doi.org/10.1016/j.pmcj.2022.101582.

Zhang, A., Lipton, Z. C., Li, M. & Smola, A. J. (2023). *Dive into Deep Learning*. Cambridge Univ. Press.

Zhang, L. & Gao, X. (2024). Transfer Adaptation Learning: A Decade Survey. *IEEE Transactions on Neural Networks and Learning Systems*, 35(1), 23–44. doi: 10.1109/TNNLS.2022.3183326.

Zhang, P., Wen, H., Zhao, Z. & Xu, Z. (2024). Time-difference reassigned transform with application to time difference of arrival for impulsive signal. *Digital Signal Processing*, 148, 104451.

Zhang, W., Liu, K., Zhang, W., Zhang, Y. & Gu, J. (2016). Deep Neural Networks for wireless localization in indoor and outdoor environments. *Neurocomputing*, 194, 279-287.

Zheng, X., Wang, C., Chen, Y. & Yang, J. (2014, Oct). Accurate rogue access point localization leveraging fine-grained channel information. *2014 IEEE Conference on Communications and Network Security*, pp. 211–219. doi: 10.1109/CNS.2014.6997488.

Zhu, H., Cheng, L., Li, X. & Yuan, H. (2023). Neural-Network-Based Localization Method for Wi-Fi Fingerprint Indoor Localization. *Sensors*, 23(15), 6992. doi: 10.3390/s23156992.

Zubow, A., Bayhan, S., Gawłowicz, P. & Dressler, F. (2020a). DeepTxFinder: Multiple Transmitter Localization by Deep Learning in Crowdsourced Spectrum Sensing. *Int. Conf. on Computer Communications and Networks*, pp. 1-8. doi: 10.1109/ICCCN49398.2020.9209727.

Zubow, A., Bayhan, S., Gawłowicz, P. & Dressler, F. (2020b). DeepTxFinder: Multiple Transmitter Localization by Deep Learning in Crowdsourced Spectrum Sensing. *Int. Conf. on Comput. Commun. and Netw. (ICCCN)*, pp. 1–8. doi: 10.1109/ICCCN49398.2020.9209727.